Friction and wear performance analysis of hydrofluoroether-7000 refrigerant as lubricant

Muhammad Usman Bhutta [a,b], Zulfiqar Ahmad Khan*[a]

[a] NanoCorr, Energy & Modelling (NCEM) Research Group, Department of Design & Engineering, Bournemouth University, Talbot Campus, Fern Barrow, Poole, BH12 5BB
[b] School of Mechanical & Manufacturing Engineering (SMME), National University of Sciences & Technology (NUST), Campus H-12, Islamabad, Pakistan
*Corresponding author: zkhan@bournemouth.ac.uk

Abstract

The disquiet about global warming has triggered the formulation and introduction of new generation of refrigerants. Hydrofluoroethers (HFEs) are within the family of newly developed environmentally friendly refrigerants with a wide range of application areas. Hydrofluoroethers reportedly have better heat transfer and thermodynamic properties. In addition to an understanding and knowledge of the thermodynamic properties of refrigerants, it is essential to understand the tribological properties of refrigerants within the context of sustainable development. Tribo-performance of refrigerants applied in refrigeration, air-conditioning and energy systems directly influences the durability, reliability and cost effectiveness of the system. HFE-7000 has considerable potential for engineering applications in green energy and low carbon technologies. In this research, a detailed investigation has been performed to assess friction and wear performance of HFE-7000 (HFE-347mcc3). HFE-7000 has been employed as lubricants. Experimental results indicate the formation of tribo-films on the topmost surfaces. Energy-Dispersive X-ray Spectroscopic (EDS) and X-ray Photoelectron Spectroscopic (XPS) analyses on the tested samples revealed significant presence of oxygenated and fluorinated anti-wear tribo-films. These oxygen and fluorine containing tribo-layers prevent metal to metal contact and contribute to the reduction of friction and wear.

Keywords: Environment-friendly refrigerants, tribo-films, sliding contact, low carbon technology, EDS, XPS.

1. Introduction

Anthropogenic global climate change, rise in worldwide economic development and the increase in global population has substantially increased the use of air-conditioning and refrigeration systems worldwide. Previous generation of artificially formulated refrigerants have high environmental implications and these refrigerants contribute towards global warming and ozone depletion [1, 2]. Although the ozone depleting refrigerants have almost been phased out, the artificially formulated refrigerants which are one of the main contributors towards global warming are still largely in use [3]. The types of refrigerants employed in cooling, refrigeration and air-conditioning systems have evolved over the years.

Naturally occurring compounds which have good heat transfer and thermodynamic properties such as Ammonia, Hydrocarbons, Sulfur Dioxide, Methyl Formate and Methyl Chloride were being used in refrigeration systems before 1930s. Almost all of these compounds are toxic, flammable or both. As a result of their use accidents were common [4]. Sulfur Dioxide, Methyl Formate and Methyl Chloride were being commonly used in domestic refrigerators which are highly toxic and highly flammable.

Several fatal accidents occurred due to methyl chloride leakage from refrigerators in 1920s [3]. This led to a collaborative research in 1928 to find alternative replacement refrigerants that would be nontoxic and non-flammable which resulted in the development of Chlorofluorocarbons and Hydrochlorofluorocarbons.

Chlorofluorocarbons (CFCs) and Hydrochlorofluorocarbons (HCFCs) were extensively used as refrigerants till the mid-1990s. CFCs are chemicals containing atoms of chlorine, carbon and fluorine. HCFCs have an additional hydrogen atom and their molecular structure resembles closely to CFCs. CFCs and HCFCs are non-toxic and non-flammable refrigerants possessing excellent thermodynamic properties. This led to the extensive use of CFCs and HCFCs in various applications including uses in residential refrigerators, domestic air-conditioning systems, commercial applications, small scale industrial and in automotive air-conditioning units. Besides having excellent thermodynamic qualities, CFCs and HCFCs also possess exceptional tribological properties [5-14]. CFCs and HCFCs were reported to form protective surface films under normal compressor operating conditions which enhanced the friction and wear of interacting parts. The discovery of the depletion of the ozone layer and publication of the destructive effects of CFCs on the stratospheric ozone layer in 1974 [15] led to the realisation that CFCs have an extremely high ozone depletion potential and are leading to the destruction of the ozone. Vienna Convention for the Protection of the Ozone layer which was followed by the Montreal Protocol on Substances that Deplete the Ozone Layer in 1987 put a ban on CFCs [16]. Montreal Protocol was enforced in 1989 worldwide which banned the use of CFCs by the start of year 1996 in developed countries. HCFCs have lower ODP (Ozone Depletion Potential) values as compared to CFCs, which has allowed their use for a longer period of time. HCFCs are planned to be phased out by the end of year 2020.

Refrigerators and air-conditioners had become common household items, bans and restrictions on CFCs and HCFCs meant that alternative refrigerants had to be introduced, however this led to the need for assessing tribo-implications of these refrigerants in turn their implications on the durability. This paved the way to the development and introduction of Hydrofluorocarbons (HFCs). HFCs are synthetically produced refrigerants which contains hydrogen atoms, fluorine and carbon with zero ODP. HFCs had thermodynamic properties matching CFCs [17-21], which resulted in their extensive use as substitute refrigerants. CFCs and HCFCs were compatible with mineral oils, HFCs however were incompatible and immiscible with mineral oils. This meant that new lubricants with various additives had to be developed for the use of HFC refrigerants in compressors. After the introduction and acceptance of HFC refrigerants various researcher around the world started investigating the tribological performance of these refrigerants. A number of tribological studies including [5, 6, 22-33] were conducted to evaluate the performance of HFC refrigerants by using a range of lubricants and additives. Numerous studies [5-11, 13, 14, 23, 34-40] were also conducted which compared the friction, wear and lubricity performance of HFCs to HCFCs and CFCs. Most of the investigations that directly compared the tribological properties of HFCs to HCFCs and CFCs concluded that CFCs and HCFCs have superior tribological performance as compared to HFCs. Fluorine in HFCs did not decompose under normal compressor operating conditions and did not form protective surface films. Having zero ODP, HFCs were deployed worldwide and their harmful global warming implications were not considered at the time of their commercialisation, however high global warming implications of HFCs were realised later. The Kyoto Protocol in 1997 to the United Nations Framework Convention of Climate Change placed limits on CO_2 and other greenhouse gases. HFCs were identified to be amongst the main contributors to global warming [41] and they will be banned in any hermetically sealed system from the year 2022.

As a response to Environmental Impact Legislations naturally occurring hydrocarbons became of interest after Kyoto Protocol. Amongst hydrocarbons, HC-600a gained particular attention as it can replace HFC-134a. Various different investigations were conducted to examine the tribological performance of HC-R600a under different testing conditions [42-49]. The study [42] showed that environmental burden is greater by using HFC-134a based systems in comparison to systems based on HC-600a. Hydrocarbon refrigerants are also considered to be up to 50% more efficient thermal conductors than fluorocarbon refrigerants [3]. However due to the inherited high flammability concerns associated with hydrocarbons their applications are limited and thus new refrigerants have to be introduced.

This has now forced the introduction of new artificially formulated alternative refrigerants. The refrigerant industry has introduced new refrigerants namely Hydrofluoroolefins (HFOs) and Hydrofluoroethers (HFEs). HFOs and HFEs have zero ODP and lower global warming potential (GWP). HFO-1234yf has thermodynamic properties matching HFC-134a and is considered a direct replacement of HFC-134a [50]. This means that HFO-1234yf can be easily introduced into HFC-134a based refrigeration cycles. Tribological evaluation of HFOs is underway and various studies [51-57] have shown that HFOs possess very good tribological properties because the fluorine in HFOs chemically reacts with the lubricants and the interacting metals to form protective tribological films on the surface. Some of these studies have also compared HFO-1234yf directly with HFC-134a under identical operating conditions and have concluded that HFO-1234yf has superior tribological properties compared to HFC-134a [51-54]. HFOs however are mildly flammable and their flammability restricts their application areas and places of use.

In recent years focus has also shifted towards refrigerants that are naturally occurring such as hydrocarbons and carbon dioxide, however the high flammability of hydrocarbons restricts their application range. CO_2 based refrigeration systems require extremely high pressures to operate which results in higher design, material and operation costs.

HFEs are non-flammable refrigerants having low GWP and zero ODP. HFEs are odourless, colourless, low toxic, low viscous refrigerants which are normally liquid at room temperature and look identical to water. HFEs have a number of applications for example they can be used in cascaded refrigeration systems, in freeze drying units, in fuels cells, in chemical reactors, in high voltage transformers, as cleaning and rinsing agents, as lubricant carriers, in vapour degreasing applications and in renewable solar thermal systems [58]. Various studies like [59, 60] have demonstrated that hydrofluoroethers possess good thermodynamics properties especially in low carbon technology and energy applications [61]. HFEs are also potential replacements of HFCs, HCFCs and PFCs [62]. There is however very limited work that has been reported on the tribological performance of newly developed HFEs. The only reported works are [63, 64]. The study [63] examined the properties of polyester in HFE-245mc atmosphere which was published back in 2002 while only the wear performance analysis of HFE-347mcc3 was performed with no comment on friction in [64].

At the time of writing this paper, no work has been published that looks into the wear as well as friction performance of 1-methoxyheptafluoropropane (HFE-7000). The study of tribo performance of this refrigerant is the novelty in this research. This is a promising new refrigerant with significant potential for industrial applications including low carbon technologies, clean energy, automotive and aerospace industries.

This study has been undertaken to experimentally evaluate the friction, wear and lubricity performance of HFE-7000 in a modified micro-friction machine. The chamber pressure and

temperature were continuously monitored and controlled to keep the refrigerant in liquid state during the testing to sustain saturated contacts. The tribological effects of load, temperature and surface roughness were studied by using Hydrofluororther-7000 as lubrication medium without using any external lubricant. A number of studies have been performed and reported in the past to investigate the tribological performance of numerous refrigerants without using any lubricants [11, 39, 43, 45, 47, 48, 53, 65-70]. Un-lubricated conditions are used to better understand the lubricity of the refrigerants by decoupling refrigerant- lubricant effects. Some of the characteristics of HFE-7000 are listed in the table 1 along with HFC-134a and HFO-1234yf. HFC-134a has a GWP value of about three times to that of HFE-7000. HFO-1234yf has a much lower GWP but is "flammable".

Table 1. Various different properties of HFE-7000, HFC-134a and HFO-1234yf [50, 53, 58, 64, 71].

Refrigerant	HFE-7000	HFC-134a	HFO-1234yf
Structure	$C_3F_7OCH_3$	Ch_2FCF_3	$CF_3CF=CH_2$
Molecular Weight (g/mol)	200	102	114
Freeze Point (°C)	-122.5	-103.3	-150
Boiling Point @ 1 atmosphere (°C)	34	-26	-29
Critical Temperature (°C)	165	101	95
Liquid Density (kg/m^3)	1400	1206	1094
Critical Pressure (MPa)	2.48	4.06	3.38
Flash Point (°C)	None	250	Not applicable
Appearance	Clear, colourless	Colourless gas	Colourless gas
Flammability	Non-flammable	Non-flammable	Mildly-Flammable
Ozone Depletion Potential (ODP)	Zero	Zero	Zero
Global Warming Potential (GWP)	530*	1430*	4*

*GWP 100-year integrated time horizon (ITH). IPCC 2013 [72].

As HFE-7000 is not considered a direct replacement of HFC-134a and it has wide range of applications areas where it can be used besides being used in compressors, this study is focusing on how the refrigerant will perform at low loads and low temperatures. Some of the studies have shown [8, 11] that refrigerants that do not form protective surface films under normal compressor operating conditions have the possibility to decompose and form surface films under severe and extremely harsh operating conditions. A refrigerant usually exists in heated vapour state in a refrigeration cycle and also undergoes a phase change; transitioning from a liquid to vapour state and when saturation temperature-pressure conditions are changed, a reversal of phase change occurs. Most of the studies involving the tribological investigation of refrigerants are concerned with the refrigerant/lubricant mixture with the refrigerant in vapour state applied in high load conditions. This study however looks into the tribological performance of one of the future generation refrigerants by experimentally assessing its performance under relatively low loads and low temperatures in liquid state without the influence of any conventional lubricant. If HFE-7000 chemically reacts with the interacting surfaces and forms protective tribo-films, it can be deduced that it demonstrates good tribological performance within the context of various operating loads and temperatures.

2. Experimental setup

Experimental configuration for conducting this research is based on an existing reciprocating micro-friction machine, Phoenix Tribology TE-57 Pressurized Lubricity Tester. The machine was modified to enable the tribological testing of the future generation of refrigerants. A modified bespoke test rig design is schematically shown in figure 1. The testing chamber houses the components under investigation. The design of the chamber allows it to be fully sealed and maintain pressures in the range of $-1\ to + 3\ bar$. O-rings and steel bellows seal the interacting components within the test

chamber to form an integral part of test chamber. All O-ring seals are static and all the relative movement is accommodated by the bellows. The setup can be used to test various contact configurations which include line contact, point contact and area contact. A ball-on-flat i.e. point contact geometry has been used for experimentation in this investigation.

The bench testing setup comprises of a variable speed PID (Proportional-Integral-Derivative) controlled DC motor. A scotch yoke mechanism is used to transmit the power from the motor to slide a lower flat plate against a fixed upper specimen in a reciprocating motion. The stroke length can be varied continuously between $1 - 5\,mm$, the frequency of oscillation can be adjusted between $2.5 - 50\,Hz$. Normal load can be applied in the range of $5 - 50\,N$. With the material samples used in this study the load range of $5 - 50\,N$ with a ball-on-flat contact configuration translates into a Hertzian Contact Stress range of $781 - 1682\,MPa$. A heater block comprising of electric heating elements is located at the bottom of the chamber which is used to heat up the refrigerant. Two K-type thermocouples are used to monitor and control the temperature of the refrigerant inside the test chamber. One of the thermocouples is directly embedded in the heater block and gives its temperature. The heater block can be heated up to 200°C. The second thermocouple is a wire type thermocouple which is secured in the specimen holding cup and is used to measure the temperature of the refrigerant under investigation. Temperature readings from the wire type thermocouple are used as feedback in a PID control algorithm to maintain the temperature of the refrigerant during the course of a test. The chamber pressure is controlled in the test chamber to keep the refrigerant in liquid state at all times during the course of a test. The test chamber is fitted with a pressure transducer and a manual pressure gauge to record, monitor and control the chamber pressure. A friction force transducer is installed to a yoke, the yoke is connected to a force feedback rod upon which a housing is mounted that holds the fixed sample. The values of the friction force and the applied normal load are used to calculate the coefficient of friction. All the parameters being controlled, monitored and recorded are displayed in real-time in the software GUI (Graphical User Interface).

All the inputs and outputs are fed through a purpose built data acquisition system which serially transmits the data to a microprocessor. The computer has a specialised software that is used to monitor, control and record the operating parameters.
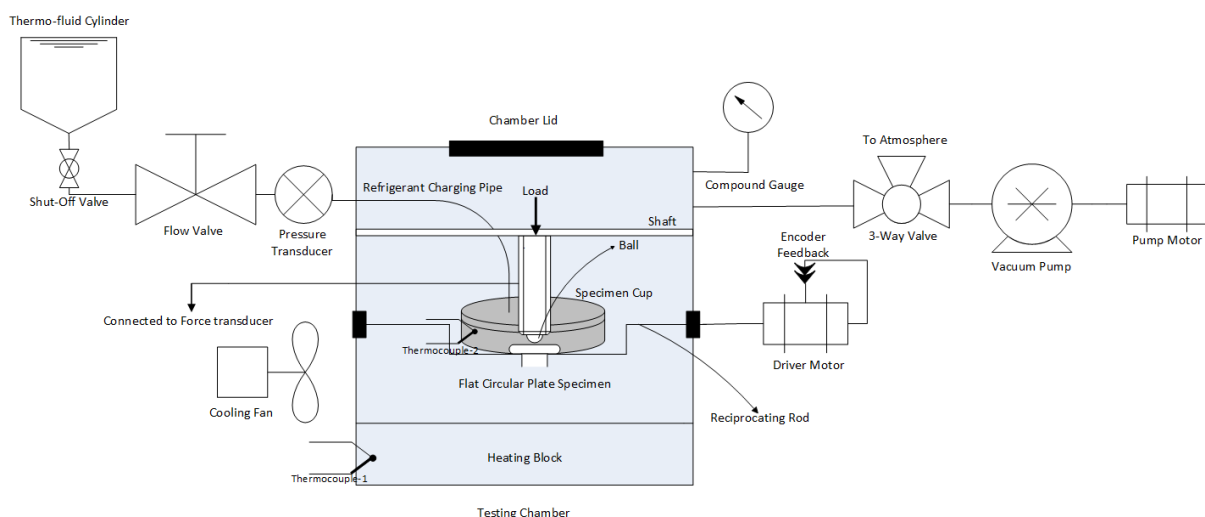

Figure 1: Test rig schematic.

3. Testing Procedure

The steel flat circular specimen is placed in the cup which is then secured on the oscillating rod with the help of screws. Then the wire type thermocouple is fastened into position. Steel ball is fixed on the ball-holder with the help of grub screws and ball holder is connected to the ball holder shaft. The shaft provides a means to secure the ball-holder in position and also functions as a means to apply the vertical normal load. After this the chamber is closed and sealed. The chamber is then vacuumed so as to minimise the effects of oxygen and ambient air during testing.

After the chamber has been vacuumed, HFE-7000 is introduced in the system by using the shut-off and flow valves. Sufficient amount of refrigerant is charged so that the cup overflows and the bottom flat specimen is fully immersed in the fluid which ensures fully lubricated conditions at all times. The extra overflown refrigerant gets collected at the bottom of the chamber where the heating block is located. This overflown refrigerant assists heat transfer from the heater block and helps maintain the refrigerant temperature in the specimen cup. The vacuum inside the test chamber and gravitational force helps the refrigerant to flow from the cylinder into the cup. The chamber lid has a transparent glass top which allows the operator to physically observe chamber conditions at all times. Next the desired load is manually applied. After this the control algorithm is run and the refrigerant inside the cup in the testing chamber is heated to the required temperature. The refrigerant temperature is controlled by using values from the wire type thermocouple and feedback PID control. Once the temperature reaches its specific value, the temperature of the refrigerant is stabilised and maintained for one hour before starting a test. After the temperature has been stabilised and has been maintained to the desired value for one hour, a test is run for two hours.

The oscillating frequency is controlled by using feedback controlled driver motor. The motor, the heater and all the transducers are connected to a microprocessor based central data acquisition and control system. The values of the friction force, the chamber pressure values, the temperature readings from the heater block, temperature of the refrigerant and the motor speed are continuously recorded in a spreadsheet.

Flat circular plate specimens of three different values of average surface roughness, $0.05\ \mu m, 0.1\ \mu m\ and\ 1\ um$ made of EN1A steel were used. The balls were made of AISI 52100 steel having an average surface value of $0.010\ \mu m$. The flat specimens are circular in shape having thickness of 2.75 mm and 30 mm diameter. The steel balls are 10 mm in diameter. Three different loads $10\ N, 20\ N\ and\ 30\ N$ were applied. Three different temperatures $20℃, 30℃\ and\ 40℃$ were used in this study. All tests were performed at a constant reciprocating of $5\ Hz$ having a stroke length of $5\ mm$. Each flat disc sample was mechanically grinded and then polished to the desired surface roughness after which each sample was ultrasonically treated with acetone for five minutes and then dried with warm air using a specimen drier before each experiment. The grinding and polishing process followed by the ultrasonic treatment with acetone of the specimens assured the removal of any unwanted/oxide surface films pre-experimentation. Each experiment lasted two hours and repeatability was ensured by conducting each experiment at least twice.

## 4. Results and discussion
4.1. Friction

Results of friction have been discussed in terms of real-time coefficient of friction values, average coefficient of friction and average frictional force. Kinematic viscosity of HFE-7000 at 20°C is

0.32 cSt, at 30°C is 0.29 cSt and at 40°C is 0.27 cSt [58]. A detailed discussion on results of friction obtained in this study is provided in sections 4.1.1, 4.1.2 and 4.1.3 respectively.
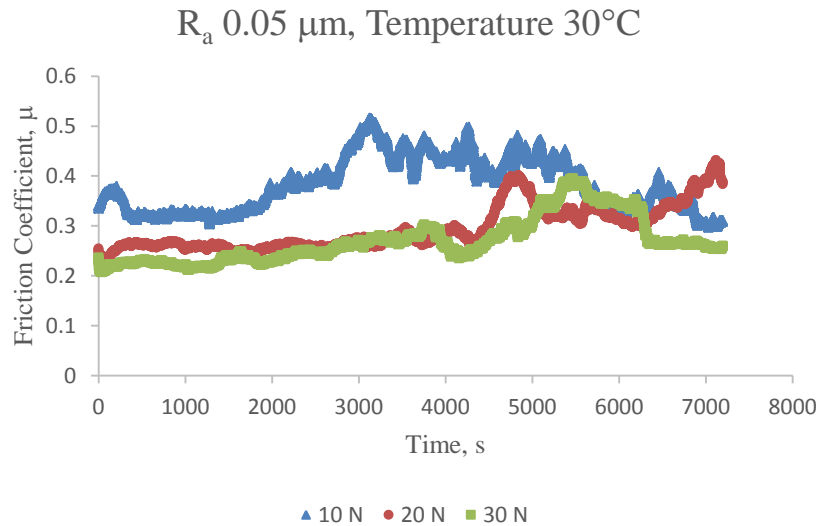
4.1.1. Coefficient of Friction

Fully lubricated conditions were established since the start of the experiment and were maintained throughout the test. The results of the variation of the coefficient of friction with changing normal load, refrigerant temperature and average surface roughness are presented in figures 2, 3 and 4 respectively.

For R_a of 0.05 μm the values of the friction coefficient decreased with an increase in load at HEF-7000 temperature of 20°C. An increase in normal load from 10 N to 30 N resulted in fewer overall variations in the coefficient of friction and more stable values. For normal load of 10 N and fluid temperature of 20°C the coefficient of friction increased almost linearly to a maximum value after which it started to decrease. With some fluctuations, the coefficient of friction decreased after increasing initially and reached a stable value at the end of the experiment. The decrease in the coefficient of friction is probably because of the development of protective tribo-films after which the coefficient of friction decreases and once the tribo-films have been formed on the entire wear track the friction coefficient reaches a stable value.

(a)
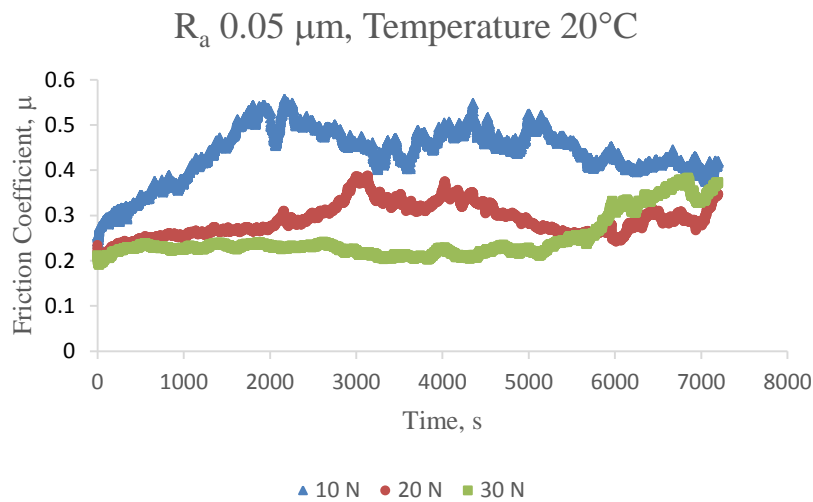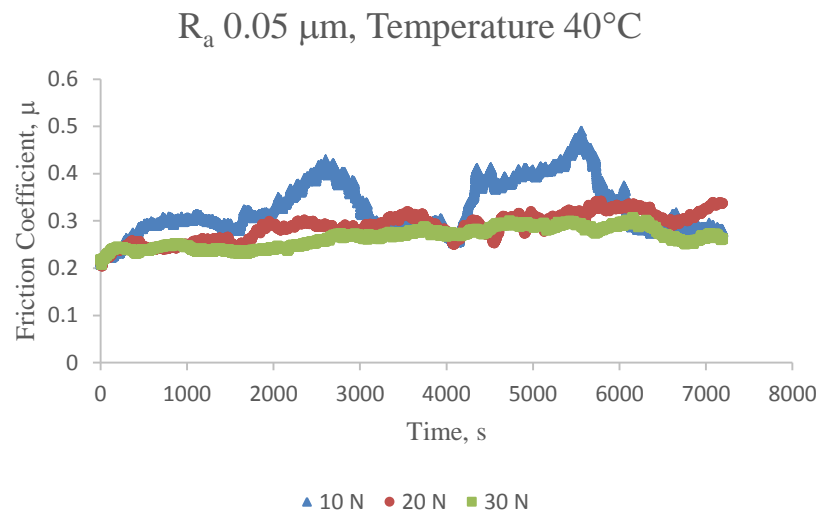
Figure 2: Coefficient of friction graphs for R_a 0.05 μm, refrigerant temperature: (a) 20℃ (b) 30℃ (c) 40℃.

For 20 N load and 20℃ fluid temperature, the overall coefficient of friction and the rate of increase of the coefficient of friction was lower as compared to 10 N and 20℃. This was probably due to the quicker formation of protective surface films.

For a load of 30 N at fluid temperature of 20℃, the friction coefficient was very stable and demonstrated a much lower coefficient of friction for over one hour of experimentation. The coefficient of friction however increased towards the end of the experiment which was due to the flattening of the ball resulting in an increase in contact area.

In comparison to 20℃, 10 N the values of 30℃, 10 N were lower. There was also no steep gradient at the start of the experiment. The friction coefficient showed similar fluctuations as 20℃, 10 N. The increase in coefficient of friction after some time is associated with the flattening of the ball and

increase in the contact area. Friction coefficient values for 30℃, 10 N decreased at the end of the experiment reaching to values which were similar to those that were at the start of the experiment.

The values for the friction coefficient for 30℃, 20 N were similar to the values of 20℃, 20 N. The values for the coefficient of friction remained fairly stable for the first hour of testing after which an increase in these values was observed. The increase in these values is associated with the flattening of the ball. The flattening of the ball increased the friction coefficient but these values reduced with the development of protective tribo-films on the freshly exposed surfaces. This stabilised the friction coefficient, however a further increase is seen at the end of the experiment indicating that the ball contact is still being flattened.

The results of the coefficient of friction for 30℃, 30 N as compared to 20℃, 30 N were also similar. The results of 30℃, 30 N followed the same pattern and had similar values as 20℃, 30 N for the first hour of testing. For the second half of the testing, a rise and fall in the friction coefficient can be observed. The rise in the values of the coefficient of friction is associated with the flattening of the ball resulting in an increase in contact area. The decrease in the friction coefficient values is due to the development of protective surface films on the freshly exposed metallic surfaces. The friction coefficient is seen to reach a low, stable and steady value at the end of the experiment.

In comparison to 20℃, 10 N and 30℃, 10 N the values of the coefficient of friction for 40℃, 10 N were lower. The values fluctuated with the passage of time but the results did not show a sharp increase in the values in the first 30 mins of testing. The values reached a stable value after the very initial increase in the coefficient of friction. The values however increased and decreased twice in the testing period resulting in the formation of two peaks. The second peek was higher than the first peak. The first peak is an indication of the initiation of the flattening of the ball and formation of protective surface films. The second peak shows a further change of the ball contact area. The value of the friction coefficient decreases and reaches a stable value at the end of the experiment demonstrating the formation of surface films on the changed contact geometries.

The overall coefficient of friction of 40℃, 20 N was similar to 20℃, 20 N and 30℃, 20 N. The values of friction coefficient showed some fluctuations but there were no major peaks and sharp gradients.
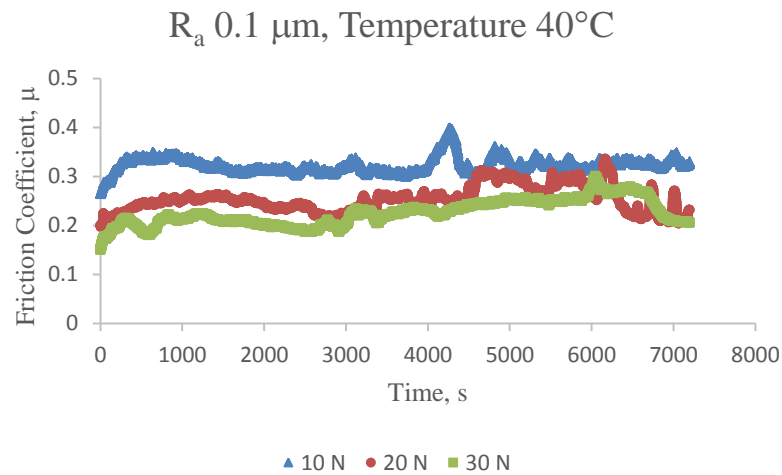
The overall coefficient of friction of 40℃, 30 N was also similar to 20℃, 30 N and 30℃, 30 N as well. The values of friction coefficient showed very minor fluctuations and presented the most stable friction coefficient from all the tests which were performed at R_a 0.05 μm.

R_a 0.1 µm, Temperature 30°C

R_a 0.1 µm, Temperature 40°C
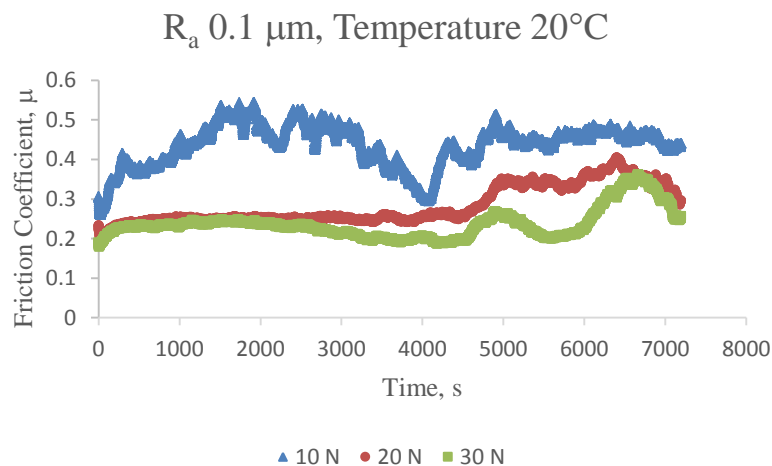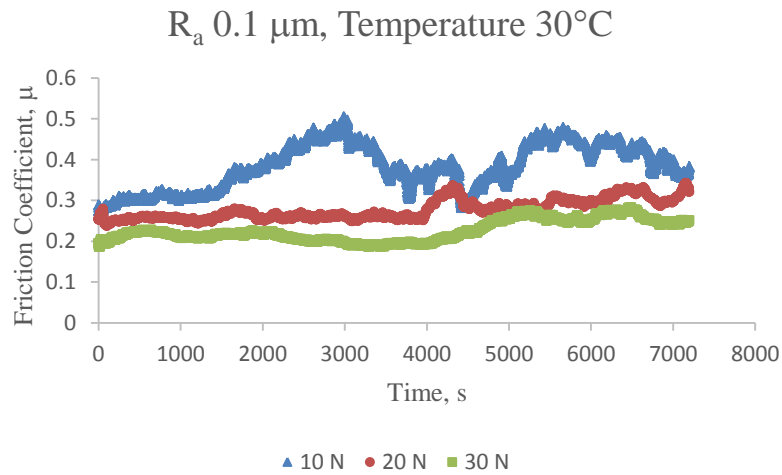
(c)

Figure 3: Coefficient of friction graphs for R_a 0.1 μm, refrigerant temperature: (a) 20℃ (b) 30℃ (c) 40℃.

For R_a of 0.1 μm the coefficient of friction displayed similar results to those obtained by using samples having R_a of 0.05 μm. For a normal load of 10 N, HFE-7000 temperature of 20℃ and R_a of 0.1 μm the variations in the coefficient of friction and the overall values of the friction coefficient were very similar to those obtained by using R_a 0.05 μm, normal load 10 N and fluid temperature 20℃. The friction coefficient showed a similar initial rise, fluctuations and then stabilisation.

For R_a of 0.1 μm, load 20 N and temperature 20℃ the initial results of the coefficient of friction are very similar to those obtained at R_a of 0.05 μm, load 20 N and temperature 20℃. The results obtained at R_a of 0.1 μm presented a stable friction coefficient for a longer time period. The friction coefficient increased after more than one hour of testing. This increase in friction coefficient was due to the flattening of the ball. A reduction in the friction coefficient can be seen at the end of the test indicating development of protective tribo-films on the freshly exposed surfaces.
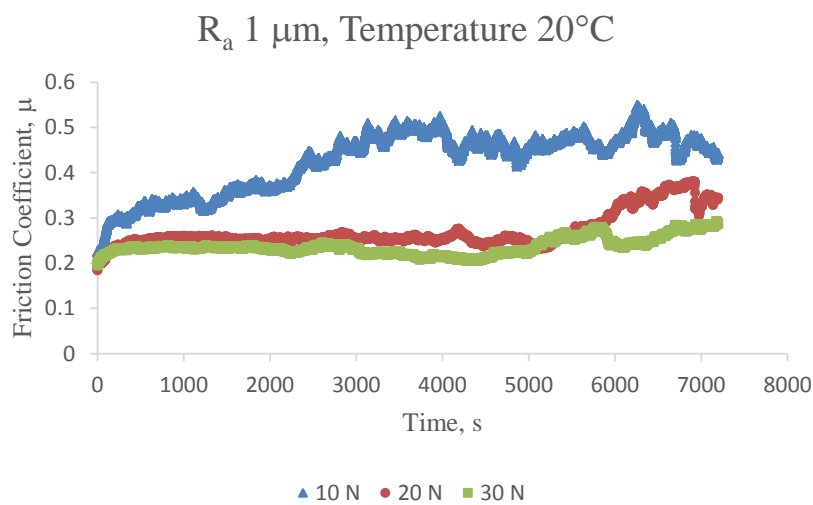
For R_a of 0.1 μm, load 30 N and temperature 20℃ the range of values of the coefficient of friction are very similar to those obtained at R_a of 0.05 μm, load 30 N and temperature 20℃. The results obtained at R_a of 0.1 μm however show two peaks indicating the flattening of the ball contact geometry. The results show that with an increase in surface roughness for the same testing conditions there were more asperity interactions resulting in quicker flattening of the ball contact. At the same time however these harsher conditions resulted in the fast formation of the protective tribo-films.

R_a of 0.1 μm, HFE-7000 temperature of 30℃ and normal loads of 10 N and 20 N showed similar results to R_a of 0.05 μm, HFE-7000 temperature of 30℃ and normal loads of 10 N and 20 N. At R_a 0.1 μm, normal load 30 N and HFE-7000 temperature 30℃ the overall coefficient of friction was lower as compared to R_a of 0.05 μm with the same load and refrigerant temperature. This shows an increase in surface roughness at higher loads is more favourable in the formation of tribo-films in turn reducing friction.

With an increase in temperature to 40℃, R_a 0.1 μm, and normal load of 10 N, the friction coefficient reduced and became more stable as compared to R_a 0.1 μm, normal load 10 N and refrigerant temperatures of 20℃ and 30℃. In comparison to R_a 0.05 μm, load 10 N and HFE-7000 temperature 40℃ the friction coefficient, in this case, was also more stable and had a lower overall value.

For R_a 0.1 μm, refrigerant temperature of 40℃ and normal loads of 20 N the friction coefficient was lower than R_a 0.1 μm, normal load 20 N and temperatures 20℃ and 30℃. The values in this case were also lower than R_a 0.05 μm, load 20 N and temperature 40℃. This indicated that increasing the temperature for the same applied load from 20℃ to 40℃ had a positive effect on the friction coefficient. This also indicates that doubling of the surface roughness at 40℃ and 20 N results in a faster formation of tribo-films and lowering of the friction coefficient.

The values for the friction coefficient at R_a of 0.1 μm, load 30 N and temperature 40℃ were lower than R_a of 0.05 μm, load 30 N and temperature 40℃. However in comparison to 20℃ and 30℃ for R_a of 0.1 μm and normal load of 30 N, the values were mostly similar.

(a)

R_a 1 μm, Temperature 30°C

▲ 10 N ● 20 N ■ 30 N

(b)

R_a 1 μm, Temperature 40°C

▲ 10 N ● 20 N ■ 30 N

(c)
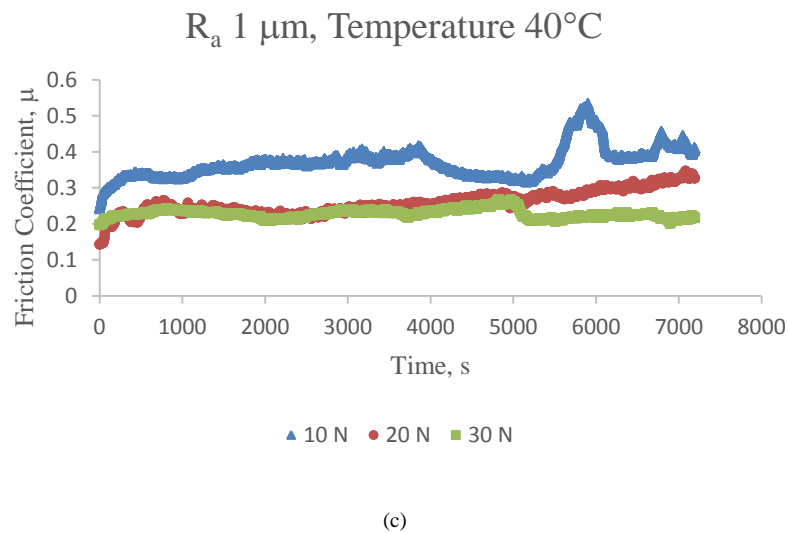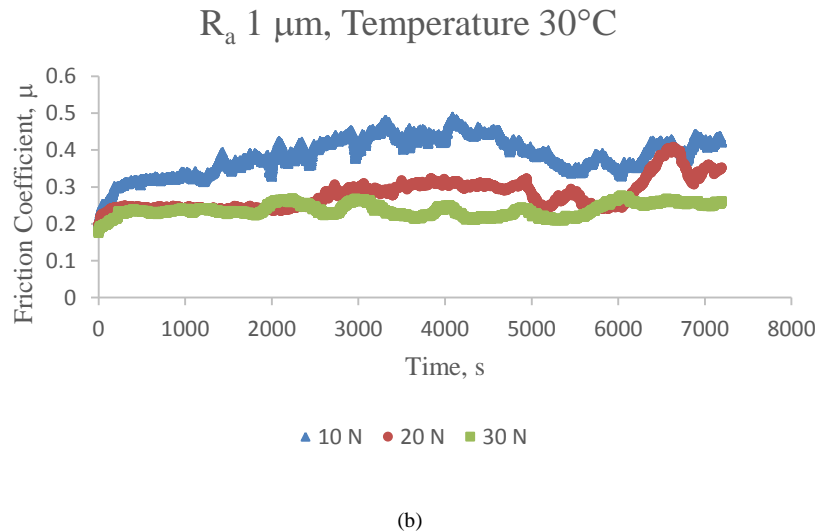
Figure 4: Coefficient of friction graphs for R_a 1.0 μm, refrigerant temperature: (a) 20℃ (b) 30℃ (c) 40℃.

A 10 times increase in average surface roughness from 0.1 μm to 1.0 μm resulted in very similar behaviour and overall values of friction coefficient in all testing conditions. The fluctuations in the friction coefficient are believed to have been caused by the generated wear debris and three body abrasive wear phenomenon. The initial fluctuations after the start of an experiment especially at lower surface roughness can also be caused by the uneven formation of the surface films, these films are believed to have been uniformly adhered after a certain amount of time which is also evident from the coefficient of friction graphs which tend to stabilise with time. The fluctuating friction coefficient is also associated with adhesive wear. The soft EN1A steel is adhered to the surface of the hard 52100 steel ball and the continuation of the reciprocating motion with adhered particles on the ball also gives rise to variations and fluctuations in the coefficient of friction.
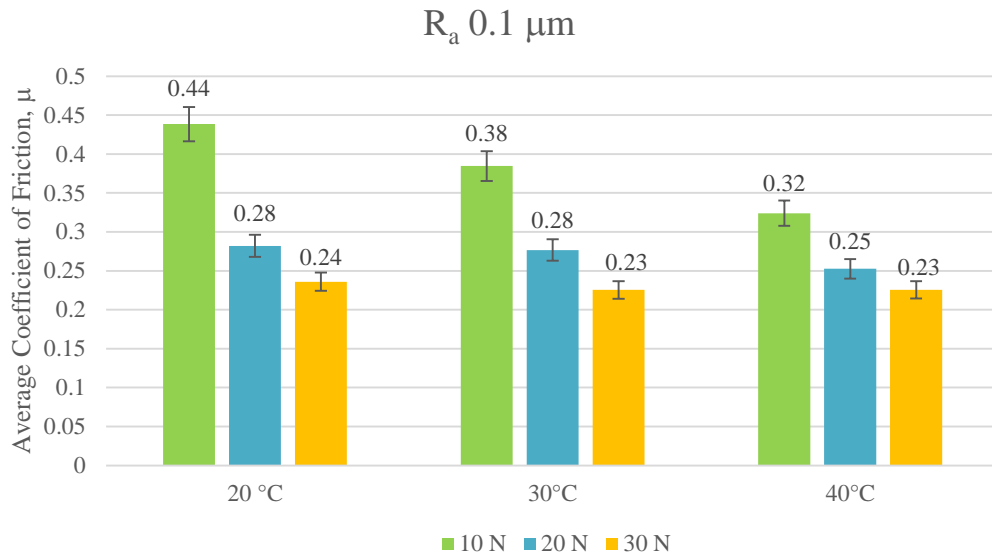
4.1.2. Average Coefficient of Friction

The results of the average coefficient of friction for all testing conditions are presented in figure 5. The data revealed a similar pattern for all investigated surface roughness values. With an increase in

load at a constant temperature the friction coefficient was reduced. Increase in load results in harsher operating environment which facilitates chemical reactions between HFE-7000 and the interacting metals. Unlike HFCs that have carbon-carbon bonds, HFEs have a carbon-oxygen bond as well which has been reported to be weaker than carbo-carbon bond [63]. The breakage of the carbon-oxygen bond and the chemical reaction between the refrigerant and freshly exposed metal produces protective tribological films on the top surfaces which reduces the friction coefficient. With an increase in temperature at the same load the coefficient of friction was also reduced. Increase in temperature at any given load reduces the viscosity of the refrigerant resulting in the reduction of separation between the rubbing components which should increase the friction coefficient due to higher asperity interactions. However the friction coefficient reduced with increase in temperature. This indicates that at higher temperatures the reactivity of HFE-7000 is increased which accelerates the formation of protective surface films. Increasing both the temperature and the load, thus results in lowering of the friction coefficient.


(a)
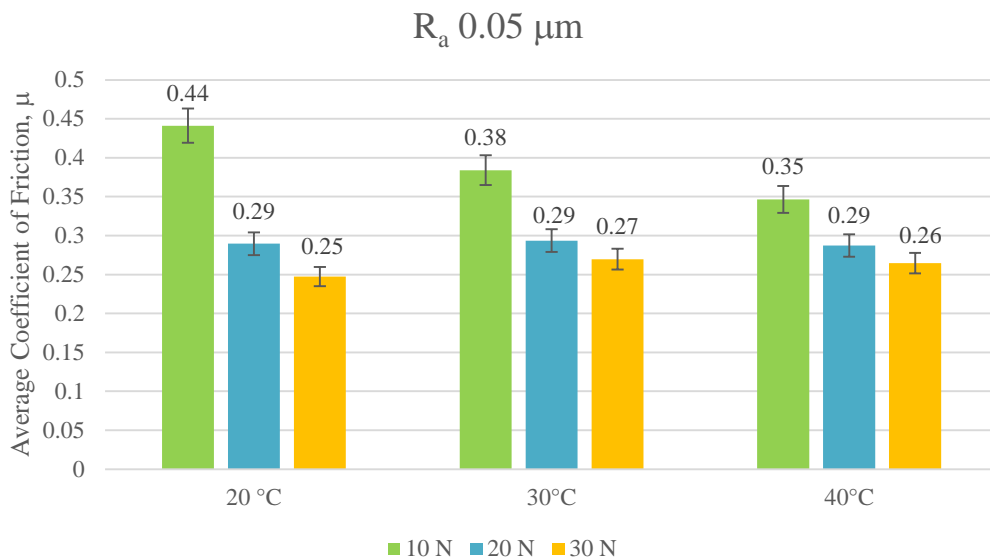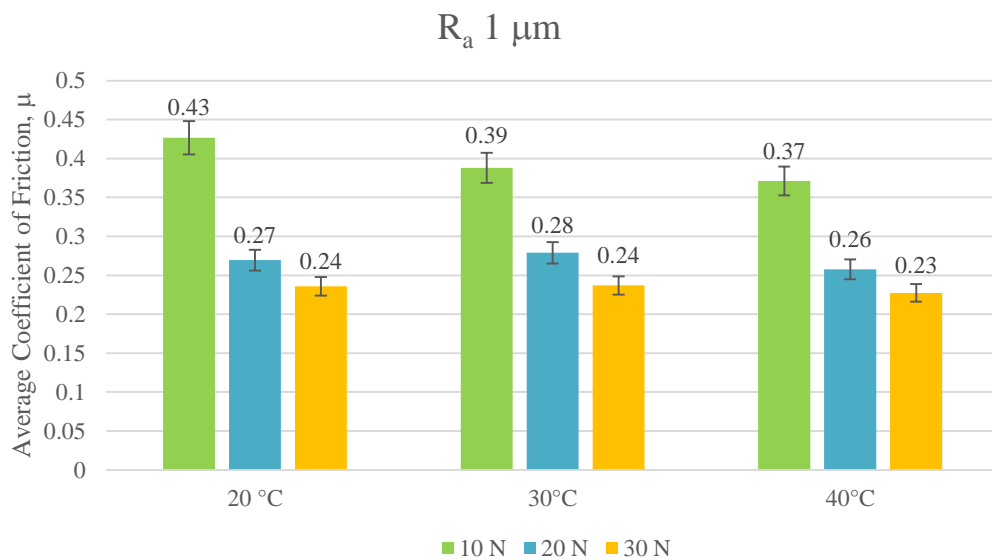
Figure 5: Average coefficient of friction plots: (a) R_a 0.05 μm (b) R_a 0.1 μm (c) R_a 1.0 μm.
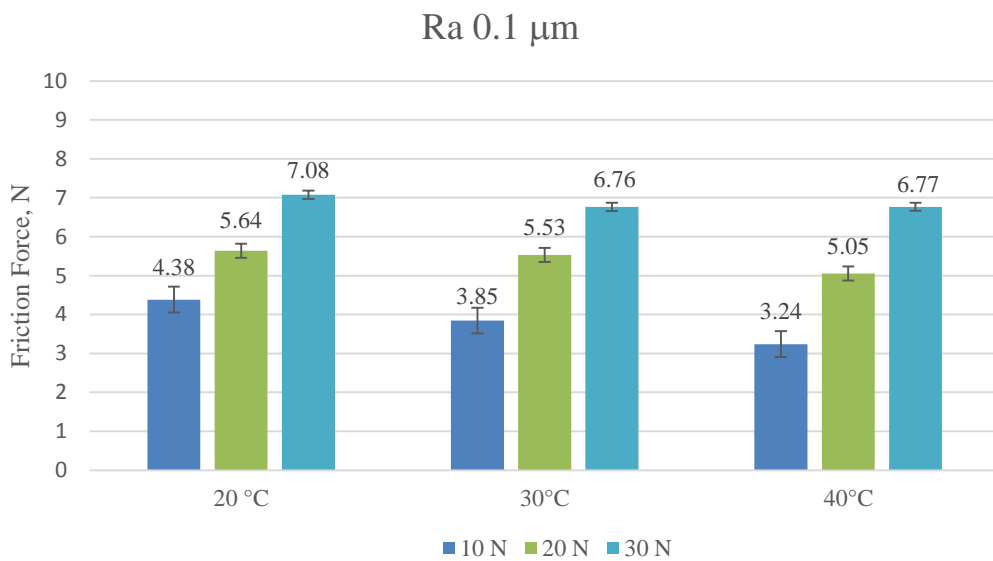
4.1.3. Average Friction Force

The results of the average friction force for all the testing conditions are presented in figure 6. The frictional force increased with an increase in load at a constant temperature for all the surface roughness values that were tested. A reduction in frictional force was observed as the refrigerant temperature was increased from $20°C$ to $40°C$ for all loads. A higher reduction in frictional force was observed with increasing temperatures for all surface roughness values at low normal load of 10 N. For loads of 20 N and 30 N the change in frictional force with an increase in refrigerant temperature from $20°C$ to $30°C$ did not have a substantial effect on the frictional force. A further increase in refrigerant temperature from $30°C$ to $40°C$ did have a positive effect on the frictional force values for 20 N normal loads. For 30 N, an increase in temperature from $30°C$ to $40°C$ resulted in a slight

reduction in the frictional force for R_a 0.05 μm and R_a 1.0 μm. For R_a 0.1 μm the frictional force stayed almost constant with an increase in temperature from 30℃ to 40℃ with 30 N normal load.
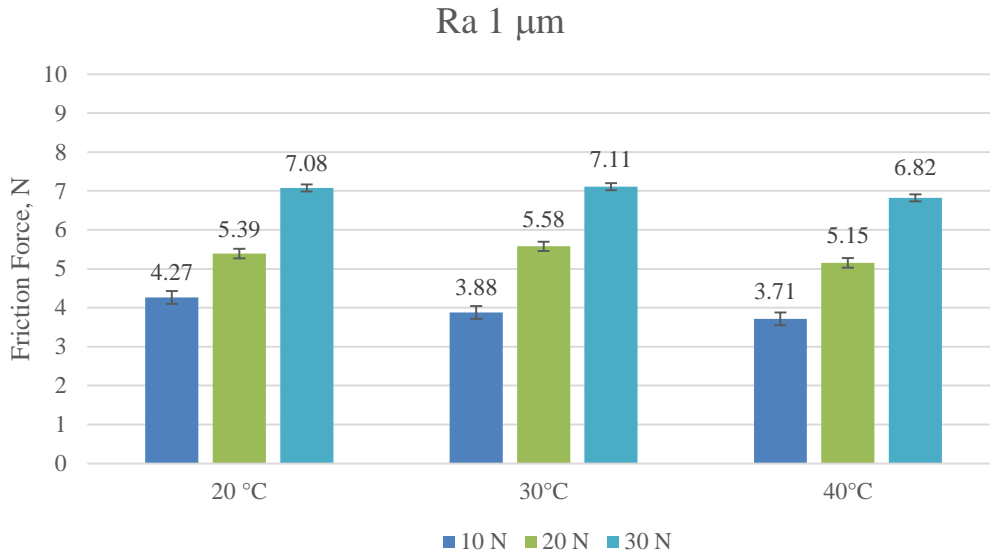
The minimum values of friction force were observed at 40℃ and R_a of 0.1 μm for all the applied loads in comparison to R_a 0.05 μm and R_a 1.0 μm. This shows that there exists an optimum value of surface roughness at which the best frictional force values are obtained when operating at higher temperatures.

(a)

(b)
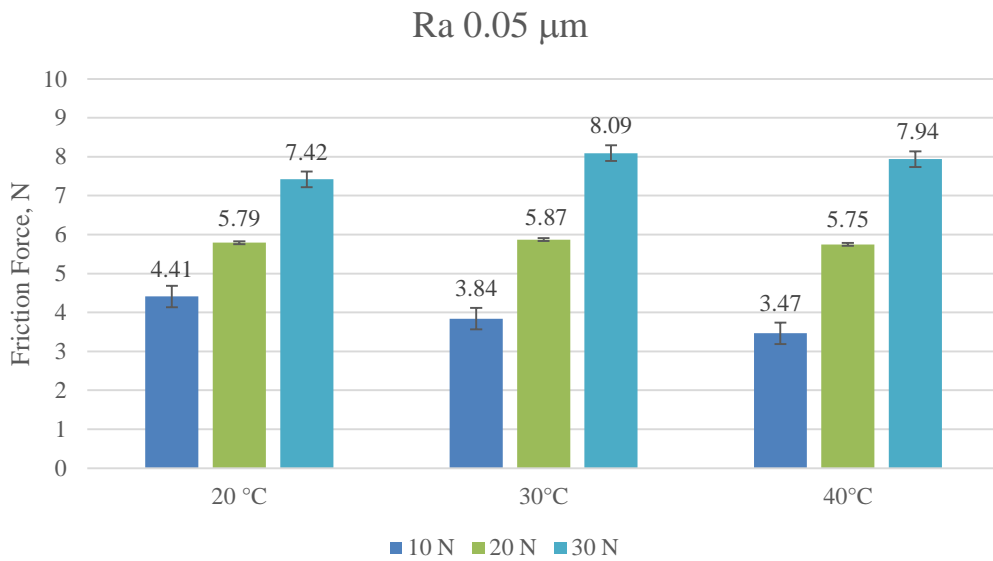
Figure 6: Average friction force plots: (a) R_a 0.05 μm (b) R_a 0.1 μm (c) R_a 1.0 μm.

5. Wear

A combination of abrasive and adhesive wear was witnessed on the flat and ball specimens. Adhesive wear mostly occurred at the ends of the wear track. Abrasive wear was more prominent in the middle section of the wear track. The soft EN1A steel was ploughed by the hard 52100 steel. Material pileup was witnessed at the edges of the wear scar. SEM (Scanning Electron Microscope) images of the flat circular specimens of average surface roughness 0.05 μm are shown in figure 7. Interestingly it was also noted that for 20 N loads for all the temperatures of the refrigerant there was less adhesive wear and more abrasive wear. Magnified images of the steel ball tested against EN1A steel having average surface roughness 0.05 μm at refrigerant temperature of 20°C and normal applied load of 10 N are presented in figure 8. The high magnification SEM images show adhered EN1A steel on the surface of the hard 52100 steel ball. Adhesive wear is believed to have been more dominant during the start of a test when the entire contact load is carried only by very small area of asperity contacts producing very high real contact pressure values, which results in detachment of fragments from EN1A steel surface and attachment to the hard steel ball under relative motion. With the flat EN1A steel sliding against the stationary hard steel ball under the influence of normal load, the adhesive junction breaks. As sliding continues fresh junctions form and rupture. When the contact geometries became more favourable after running-in of the components is achieved and after the initiation of the formation of tribo-films the wear mechanism shifts towards abrasive wear. Generated wear debris result in three body abrasive wear phenomenon as they are trapped inside the flat specimen and refrigerant holding cup. The reciprocating motion causes material pileup on the sides and ploughing of EN1A steel by the hard steel ball. Similar results were seen by observing the other surface roughness values tested under Scanning Electron Microscope as well.
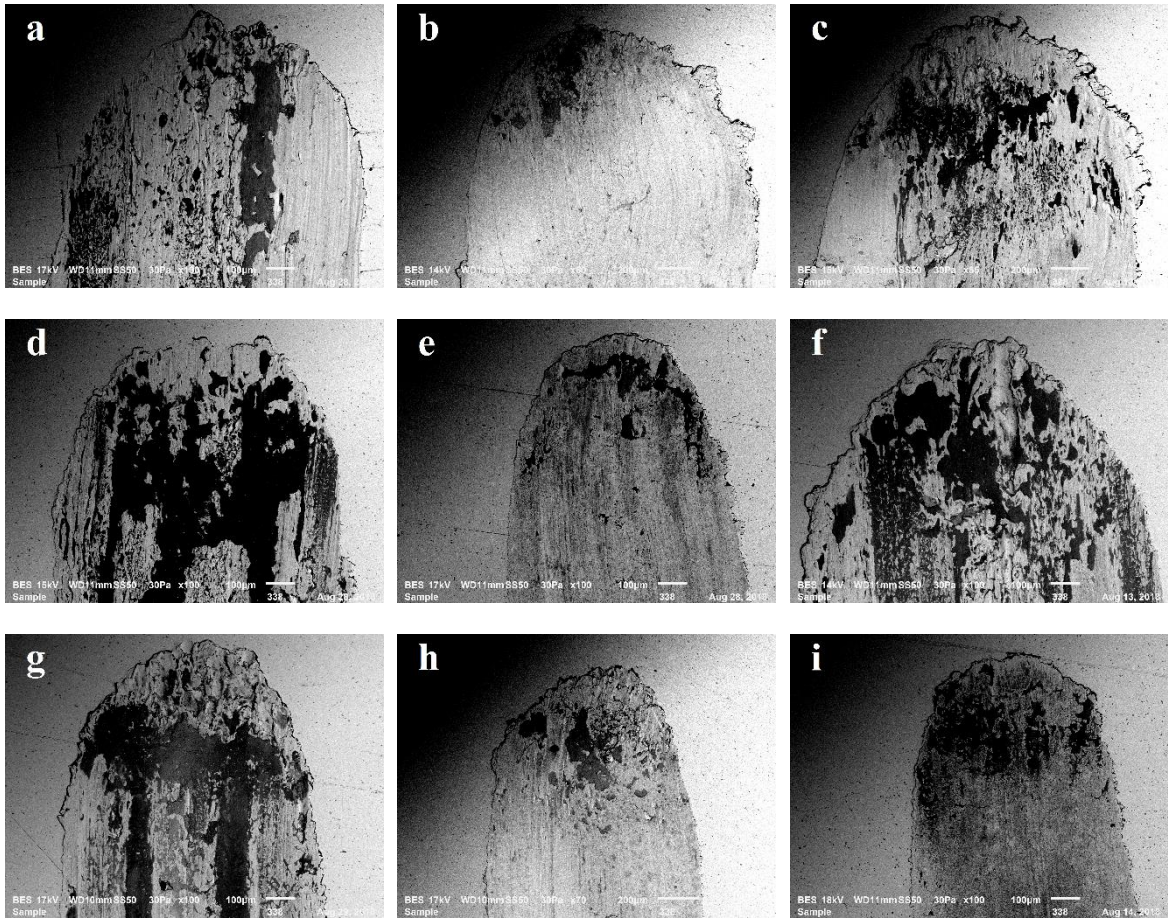
Figure 7: (a) $10\ N, 20°C$ (b) $20\ N, 20°C$ (c) $30\ N, 20°C$ (d) $10\ N, 30°C$ (e) $20\ N, 30°C$ (f) $30\ N, 30°C$ (g) $10\ N, 40°C$ (h) $20\ N, 40°C$ (i) $30\ N, 40°C$
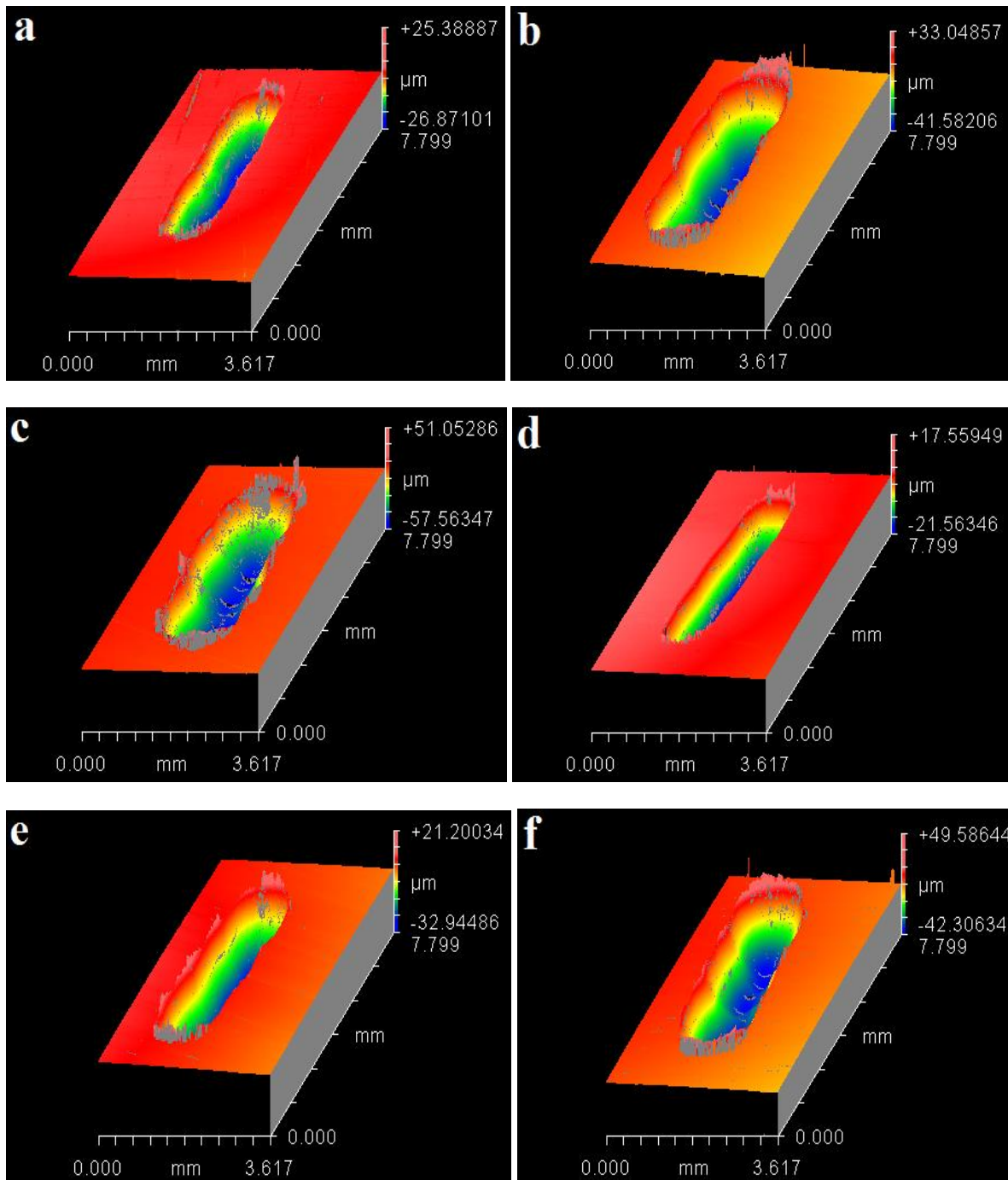

Figure 8: (a) Magnified images of the ball sample tested at $10\ N, 20°C$.

5.1. Wear Volume

Flat disc samples were also analysed under a white light interferometer to generate 3D plots. 3D plots obtained by using the interferometer were used to compute the wear volume for each sample tested. 3D oblique plots for all the tests that were conducted during this research on $0.05\ \mu m$ are shown in figure in 9.

For HEF-7000 temperature $20°C$, an increase in load generates a deeper and wider wear track resulting in increased wear volume. This pattern is also observed at $30°C$ fluid temperature, increasing load produces more wear. It can also be observed from the plots that increasing temperature from $20°C\ to\ 30°C$ at any given load reduces the depth and width of the wear track thus lowering wear.

HFE temperature $40°C$, $20\ N$ load generated the shallowest wear tracks. Compared to $20°C$ and $30°C$, wear tracks are less deep at $40°C$ at any given load.
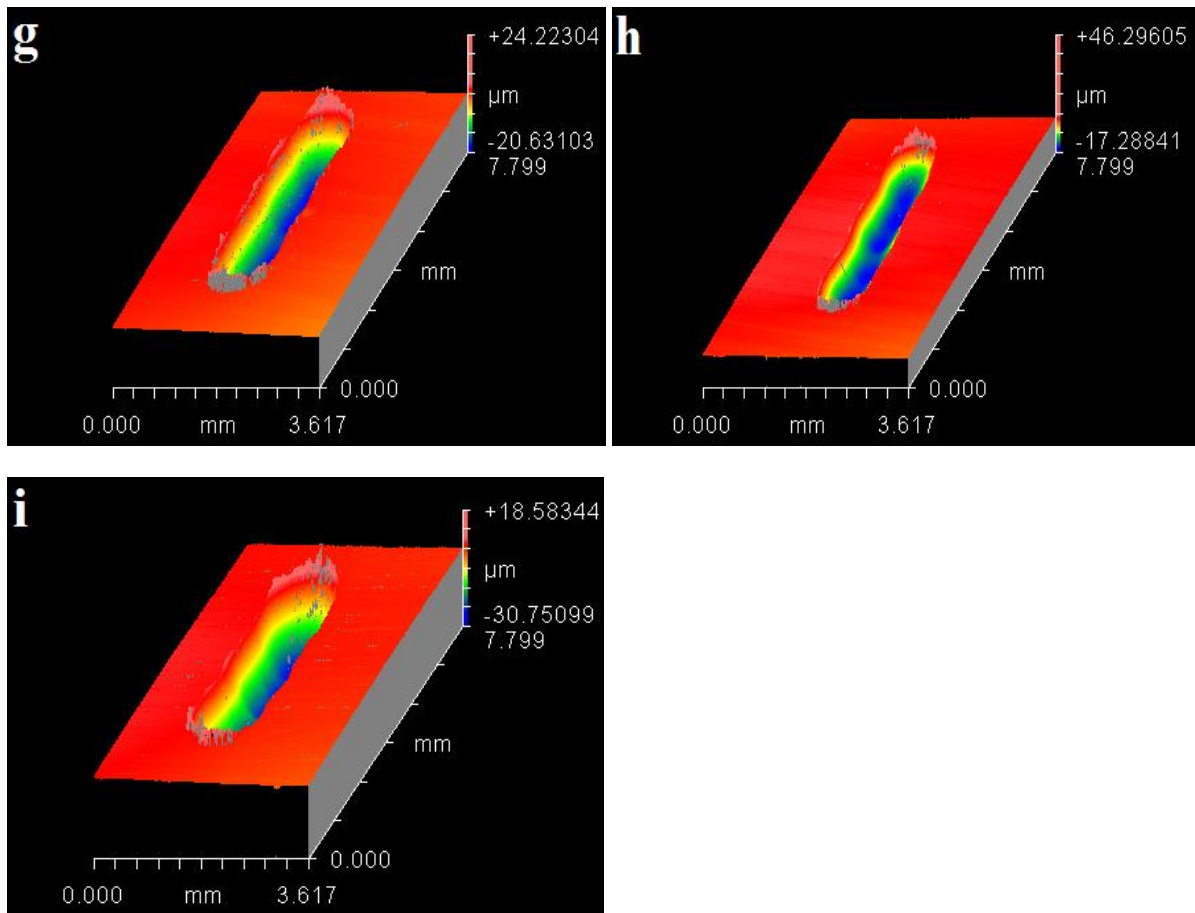
Figure 9: (a) $10\,N, 20℃$ (b) $20\,N, 20℃$ (c) $30\,N, 20℃$ (d) $10\,N, 30℃$ (e) $20\,N, 30℃$ (f) $30\,N, 30℃$ (g) $10\,N, 40℃$ (h) $20\,N, 40℃$ (i) $30\,N, 40℃$

Wear volume for all the flat samples tested was measured and the corresponding results are presented in figure 10. For a given surface roughness, a rise in temperature has a positive effect on decreasing the wear volume for the same applied load. This means that an increase in temperature increases the reactivity of the HFE-7000 with the interacting surfaces in turn resulting in a faster development of protective surface films which help decrease wear. For all the tested surface roughness values the amount of wear increases with an increase in load for temperatures of 20℃ and 30℃. At 40℃ the wear volume at 20 N is less than the wear volume at 10 N, at 30 N the wear volume has the highest value for all surface roughness values. This shows that there exists an optimum combination of load and temperature which results in lesser wear.
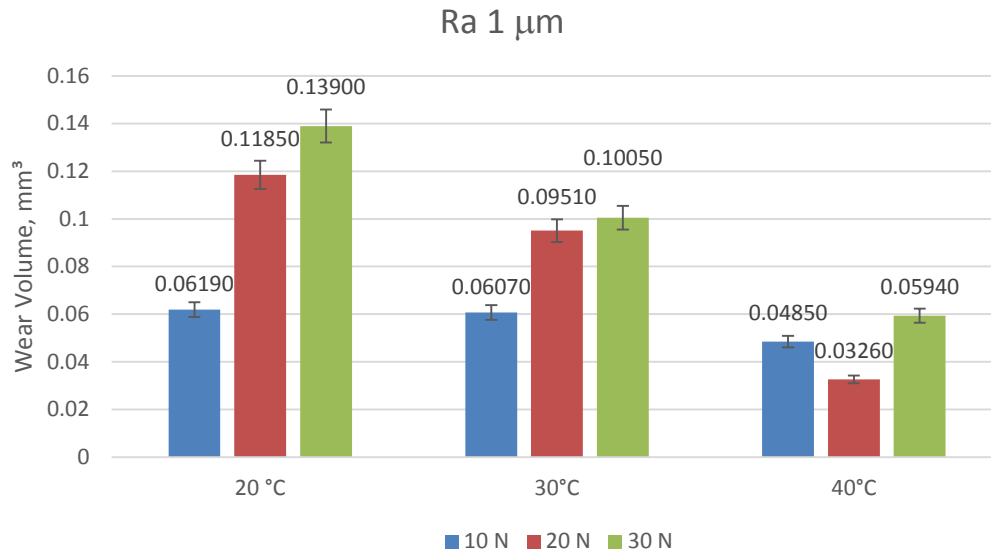
(a)

(b)
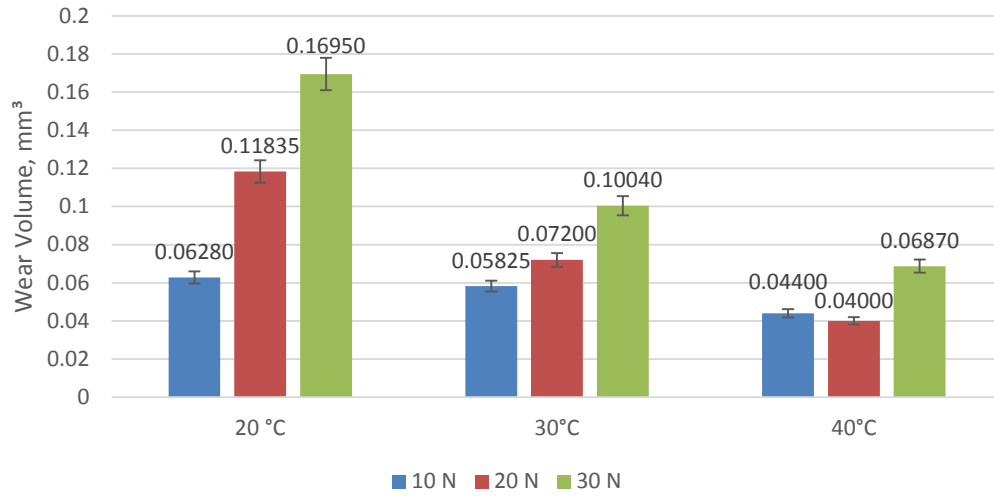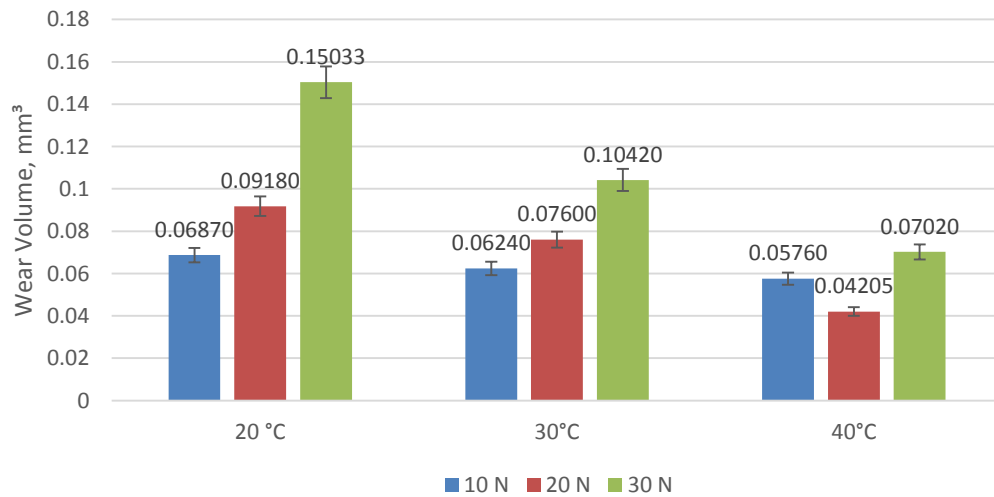
Ra 1 μm

At a load of $10\ N$ for all the tested temperatures an increase in average surface roughness from $0.05\ \mu m\ to\ 0.1\ \mu m$ generates more wear. Further increasing the surface roughness from $0.1\ \mu m\ to\ 1.0\ \mu m$ showed a reduction in wear volume for normal load of $10\ N$ at each temperature. Minimum wear for $10\ N$ load was observed at the least rough surface. These results indicate that increasing the surface roughness at lower loads increases wear due to increase in asperity interactions. Further increasing the surface roughness results in harsher operating conditions creating more asperity interactions, these conditions however proved to be more favourable for the chemical breakdown and reaction of HFE-7000 with the metallic surfaces producing protective surface films decreasing wear.

An increase in load from $10\ N\ to\ 20\ N$ at $20°C$ showed almost the same values of wear volume for $R_a 0.05\ \mu m\ and\ R_a 1.0\ \mu m$, however at $R_a 0.1\ \mu m$ wear volume showed the least values for $20°C\ and\ 20\ N$. This shows that for $20\ N\ and\ 20°C$ there exists an optimum value of surface roughness which will result in lower wear. For $20\ N$ load $30°C$ conditions the wear volume increases with an increase in surface roughness. For $20\ N$ and $40°C$ the wear volume increased with an increase in surface roughness from $0.05\ \mu m\ to\ 0.1\ \mu m$, however at $R_a 1.0\ \mu m$ least values of wear volume was noted. This indicates that although hasher conditions promote the production of surface tribo-films, the temperature has to increase as well to accelerate the formation of these films. $20\ N, 40°C$ testing condition for each surface roughness produced the least amount of wear. The wear volume was lower than $10\ N$ loads. This indicates that an optimum combination of load and temperature exists which produces least wear irrespective of the surface roughness. Testing conditions of $R_a 1.0\ \mu m$, HFE-7000 temperature $40°C$ and normal load of $20\ N$ produced least overall wear showing the best operating conditions.

For $30N$ load at $20°C$ an increase in surface roughness resulted in a decrease in wear volume. At $30°C\ and\ 30\ N$ load an increase in surface roughness did not have any noticeable effect on the wear volume. Increasing surface roughness at $30\ N, 30°C$ resulted in almost the same wear. At $30\ N, 40°C$, an increase in surface roughness from $0.05\ \mu m\ to\ 0.1\ \mu m$ increased wear, but increasing surface roughness to $1.0\ \mu m$ reduced wear and resulted in the least wear volume for these testing conditions.

6. Tribochemistry Discussion

Post experimental Energy-Dispersive X-ray Spectroscopic (EDS) analyses were carried out in a vacuumed chamber on *all* the specimens tested. A strong presence of F and O was detected on *all* of the flat circular specimens as well as on *all* of the steel balls. EDS analysis was also conducted for a selection of the specimens before experimentation. As each sample was grinded, polished and ultrasonically conditioned with acetone pre-experimentation, no oxygen or fluorine was detected on the samples pre-experimentation. X-ray Photoelectron Spectroscopy (XPS) analysis was carried out on a number of sample pairs to study the surface composition post experimentation. EDS results of one of the specimen pairs tested are shown in figure 11 and figure 12 respectively.
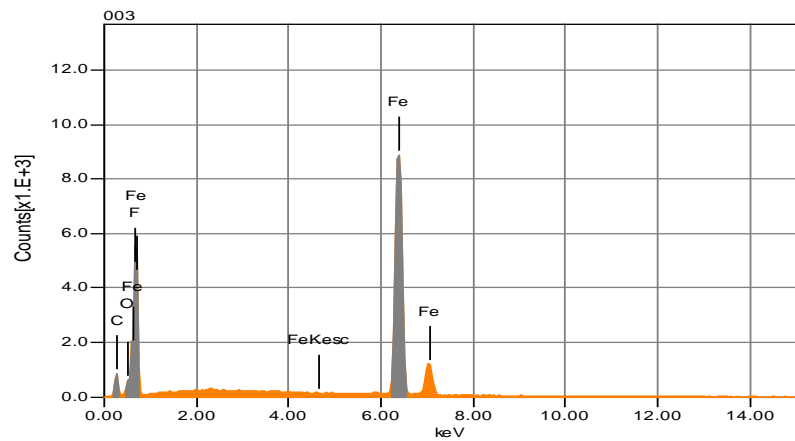
(a)
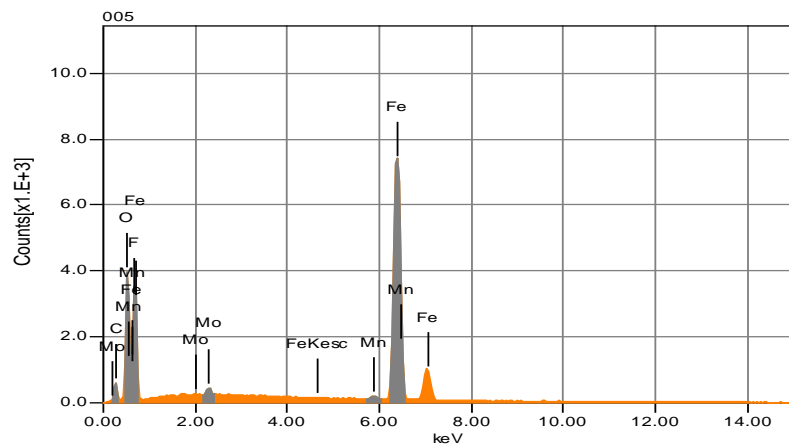
(b)
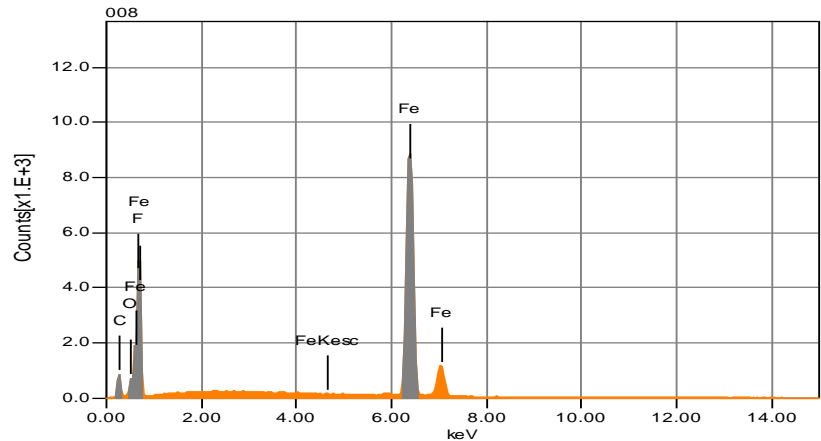
(c)

Figure 11: Magnified images of the wear scar indicating the analysis region along with the EDS analysis.

Figure 11 shows the magnified image of a wear scar on the EN1A steel flat circular specimen along with the chemical characterization results obtained by analysing different regions on the wear track. Similar results were obtained for the other flat specimens as well. Different regions on the wear track were examined which revealed the presence of both oxygen and fluorine on the wear track indicating the development of tribo-films on the wear scar.

Figure 12 shows the elemental analysis of the 52100 steel ball. The analysis on the ball was also performed at various different regions within the contact zone. The analysis also revealed the presence of both oxygen and fluorine demonstrating that the protective surface tribological films were not only formed on the flat specimen were also formed on the ball specimen as well.
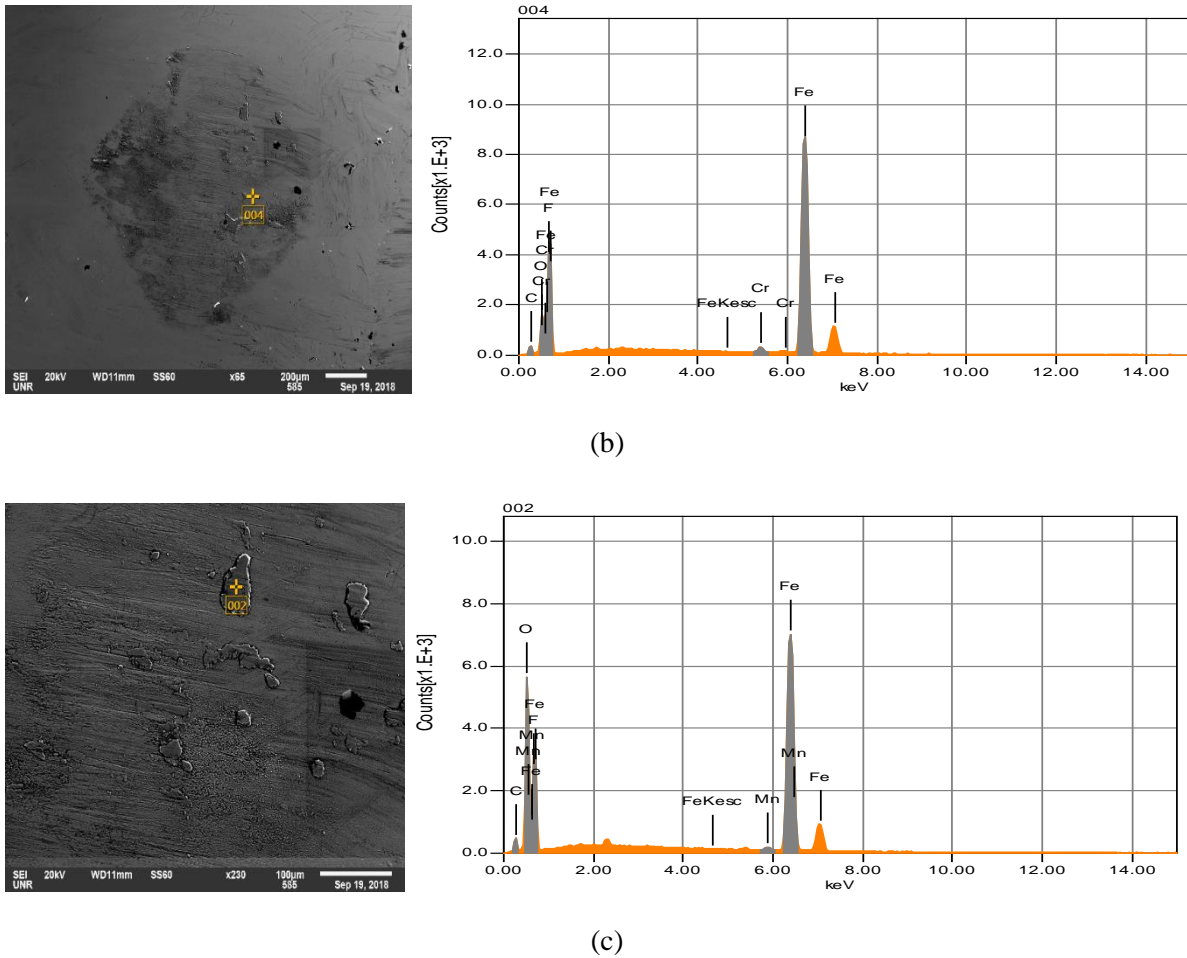

(a)

(b)

(c)
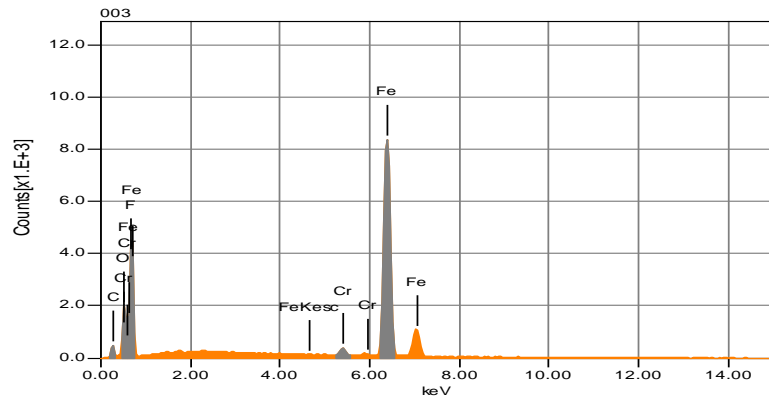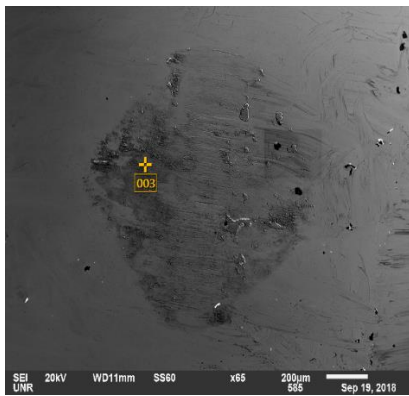
Figure 12: Magnified images of a ball specimen indicating the analysis region along with the EDS results.

The experimentation chamber was vacuumed to minimise the effect of ambient air before introducing the refrigerant in the system and establishing fully lubricated conditions after which the test chamber was sealed, which means that the origin of post experimentation detected oxygen and fluorine is the refrigerant. The samples were stored in a desiccator after experimentation. Even if aerial oxidation is taken into consideration while handling and transporting the sample post-experimentation still will not explain the detection of high percentage of fluorine and oxygen on the surfaces of the tested samples.

X-ray Photoelectron Spectroscopy (XPS) was performed in ultra-high vacuum using a Kratos Axis Ultra photoelectron spectrometer (Kratos, Manchester, UK). A monochromated aluminium X-ray source was operated at 15 kV, 10 mA emission illuminating at 60º to the sample surface normal. Each analysis performed had an approximate area of $700 \, \mu m \times 300 \, \mu m$. The analysis conditions used were: 160 eV pass energy, 1 eV steps and 0.2 s dwell per step. Survey spectra in the range of 1350 to - 10 eV binding energy were taken at 0° emission angle to the surface normal of the sample. The XPS survey spectra results of one of the sample pairs tested are shown in figure 13. Besides iron, carbon, silicon, manganese, sulphur, phosphorus and chromium which are typically present in EN1A steel and 52100 steel, trace elements such as sodium, zinc, calcium, magnesium, fluorine and nitrogen were also detected. The source of sodium, zinc and calcium is believed to be the nitrile and latex laboratory rubber gloves which were used for sample handling. Numerous components within a glove material and manufacturing residues left on the surfaces of gloves have been reported to be easily transferred to other materials with zinc, sodium and calcium being a common contamination caused by laboratory gloves [73].
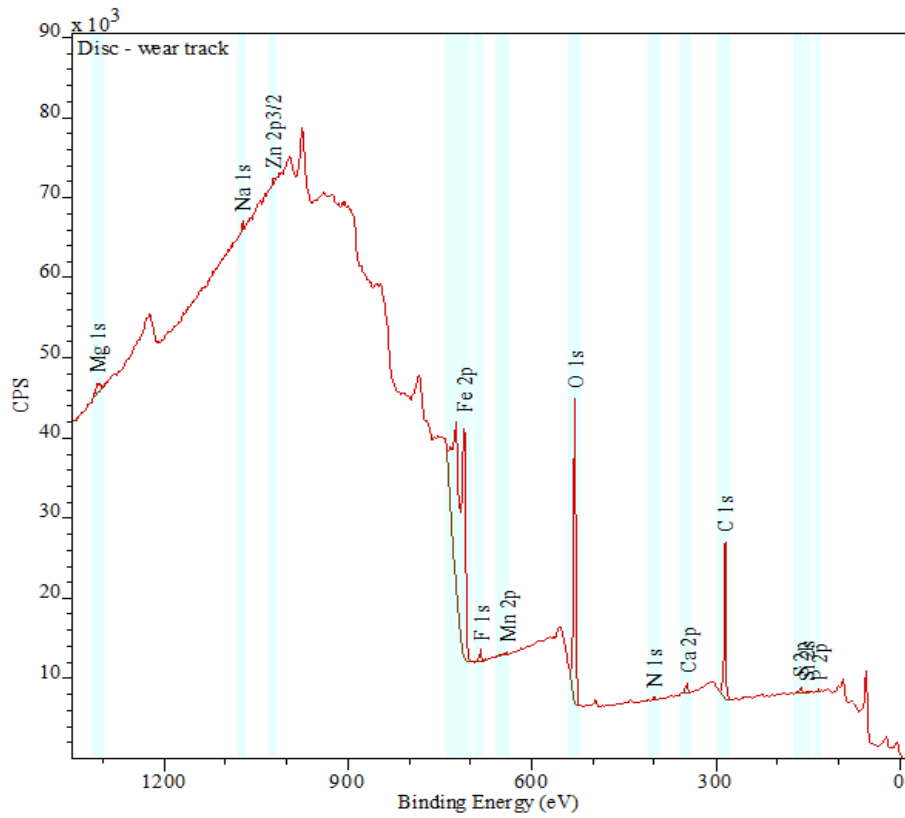
(a)
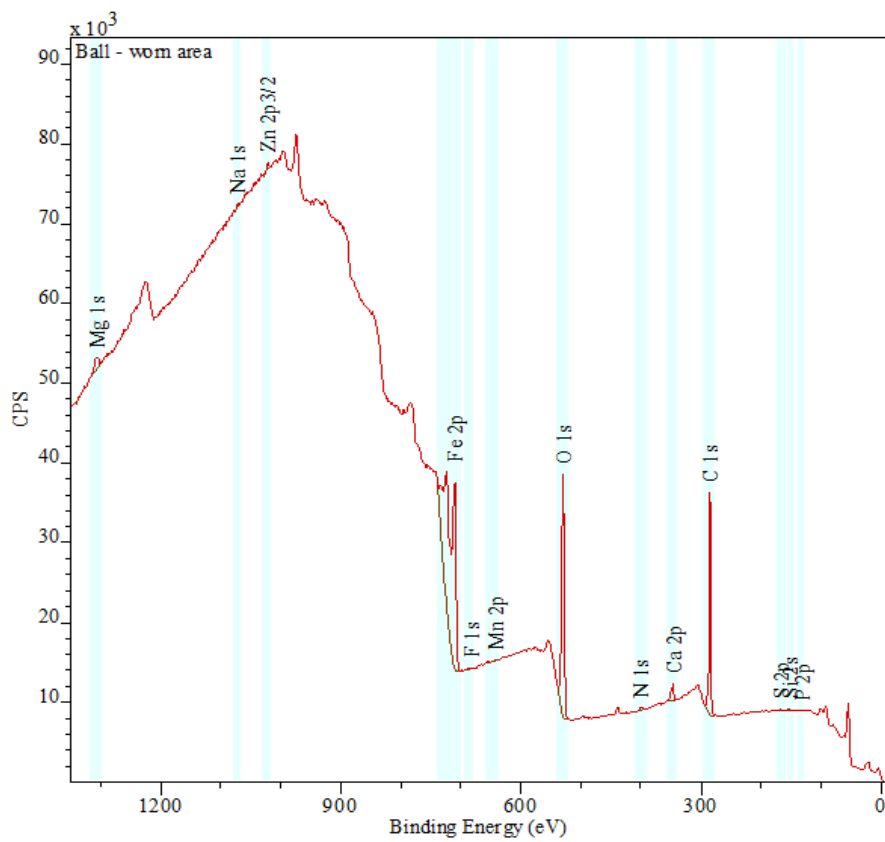
(b)

Figure 13: XPS survey spectra: (a) Disc (b) Ball

Nitrogen is often associated with carbon contamination from the atmosphere and this is consistent with the inelastic background of the C 1s peak which indicates that it is mainly a contaminant overlayer. Elements of interest i.e. the constituents present in the refrigerant and steel samples were further investigated and are presented in figure 14.

Figure 14 shows the XPS high resolution core level spectrum results for iron, carbon, oxygen and fluorine. Figure 14 (a) shows the Fe 2p high resolution core level spectra for the ball and flat circular disc. The binding energy peaks of Fe $2p_{3/2}$ at 710.7 eV for the ball as well as the flat sample are present in the results which we assign to the formation of Fe_2O_3 [74]. A small $2p_{3/2}$ peak at ~ 706.7 eV is also present in the spectra which indicates Fe metal [74]. Compared to the metal, iron oxide peaks are significantly shifted to a higher binding energy [74].

Figures 14 (b) and 14 (c) illustrate the C 1s high resolution core level spectra of the flat circular disc and the ball specimens respectively. The results of the C 1s spectra for the flat disc sample can be fitted using four different peaks with respect to the results shown in figure 14 (b). With reference to figure 14 (c), the C 1s XPS spectrum obtained for the ball specimen is very similar to the flat sample expect for the fact that the ball spectrum can be fitted using three different peaks instead of four. This implies that similar carbon constituents are present on both the samples, with an additional carbon compound present on the flat disc. The peaks with binding energies between 285.0-285.3 eV are present on both the samples. Of the total percentage of C 1s intensity detected from the analysed area on the disc, 80.1% of it is present within these peaks. For the ball sample, 84.5% of the C 1s intensity lies within these peaks in the area analysed. For adventitious carbon contamination C-C typically has binding energy of 284.8 eV [74]. The analysis process has an inherited error of at least ± 0.1 eV to ± 0.2 eV [75]. It is convenient, for electrically insulating systems to use the C-H, C-C signal as a binding energy reference and set it to 285.0 eV [75]. Further high binding energy components can be identified above this main peak. +1.6 eV above the C-H, C-C peak is consistent with carbon singly bonded to oxygen, C-OH and C-O-C [74, 75]. The peak at+2.8 eV above the C-H, C-C peak is typical of C=O [75], this third peak is found in the fit of the data from the flat sample and not on the ball. The fourth peaks which are in the range of 288.7-288.9 eV is typical of O-C=O [74, 75]. The binding energies in the range of 288-290 could indicate the presence of metal carbonates [75]. The detection of peaks in the C 1s spectra on the worn regions within these (288-290 eV) binding energies could possibly also mean the formation of iron carbonates. The results of the C 1s spectra for the flat as well as the ball sample indicate the presence of multiple carbon based compounds showing that not only the bonds of the refrigerant have broken but also new bonds have been formed.

The O1s spectrum obtained by analysing the flat disc and ball specimen are shown in figures 14 (d) and 14 (e) respectively. Similar to the C1s spectrum, O1s spectrum for the ball and the flat samples show similar peaks. Multiple peaks are generated at binding energies 529.8 eV to 529.9 eV and 531.5 eV to 531.8 eV for the disc as well as the ball specimens. This indicates that similar oxygen constituents are present on both the tested samples. For the area analysed on the disc, 68% of oxygen contributes to a peak at 531.5-531.8 eV and 32% of the O 1s intensity is in a peak centred at 529.8-529.9 eV. For the ball sample, 64.2% of the O 1s intensity is in a peak at 531.5-531.8 eV and 35.8% is in in a peak at 529.8-529.9 eV. Besides metal oxides, the O 1s binding energy of various species and compounds lies within a very narrow range [74]. Interpretation of the O 1s spectra is not straightforward as O 1s peaks are broader with multiple overlapping components [74]. Binding energies in the range of 529-530 eV are typical of metal oxides, in this case and consistently with the

Fe 2p binding energies, most probably Fe_2O_3 [70, 74]. Fe_2O_3 is the mostly likely metal oxide to have formed as Iron (III) Oxide was directly detected in the Fe2p spectra. The binding energies in the range of 531.5-532 eV imply the presence of C-O [74], C-O was also detected in the C 1s spectra. For the O 1s spectrum, binding energies in the range of 531.5~531.9 could also indicate the formation of carbonates and/or bicarbonates [70, 76]. The possible formation of metal carbonates was also detected in the C 1s spectrum. Oxygen bonded to organic components can range in binding energy from as low as 530.9 eV to as high as 533.8 eV and metal hydroxides are reported to have a binding energy of 531.3 eV with a standard deviation of 0.3 eV [75]. The most likely metal hydroxides, if present, could be $Fe(OH)_2$ and $Fe(OH)_3$. The results show that a higher percentage, more than 60% of the oxygen detected is bonded to organic components or possibly in the form of metal hydroxides. The rest of the oxygen is in the form of metal oxides with Fe_2O_3 being the mostly probable metal oxide formed on the surface.

The F 1s spectrum for the disc and ball specimens is presented in figure 14 (f) and figure 14 (g). Unlike the previous XPS results, the F1s spectra for the ball and the disc are different. 81.7% of the fluorine detected on the disc sample is at 684.4 eV binding energy while 18.3% of fluorine was identified at 688.2 eV binding energy. For the ball specimen, a peak was only detected at ~684.5 eV. For fluorine F1s spectra the binding energies from 684 eV to 685.5 eV indicate the presence of metal fluorides [74] and from 688 eV to 689 eV is more typical of organic fluorides. A peak was detected in the range of 684 eV to 685.5 eV while no peaks were detected for the ball sample in the range of 688-689 eV, which means that only metal fluorides are present on the ball sample on the area analysed and fluorine is not present in organic state. For the disc sample a very high percentage (81.7%) of fluorine is present as metal fluorides, while a smaller percentage (18.3%) is present as organic fluorine. The presence of metal fluorides and organic fluorine also suggests that the bonds in the refrigerant have been broken and new bonds have been formed on the surfaces of the rubbing metals. These results are in contrast to the results of oxygen. Oxygen is present in a higher percentage in organic form while a smaller percentage of oxygen is present as metal oxides as discussed in the O1s spectrum results. In addition metal fluorides are present on both the samples while organic fluorine is present only on the disc sample. This indicates that fluorine in HFE-7000 has a higher tendency to form metal fluorides in comparison to oxygen in HFE-7000 to from metal oxides. The metal fluorides are most probably FeF_2 and/or FeF_3 [53, 54, 63] or mixed iron oxyfluorides.

The detection of inorganic compounds such as iron (III) oxide and metal fluorides originate from the tribochemical reaction between the steel ball/disc and the fragmented species coming from the HFE-7000 refrigerant breakdown. The organic species have been reported to act as the third body ensuring sustainability of the interface in terms of wear and friction, whereas the metallic components (fragmented refrigerant reacted with steel) on the other hand provide better adhesion on the surfaces of the rubbing metals [54].

(a)

(b)

(c)

(d)

(e)

(f)

(g)
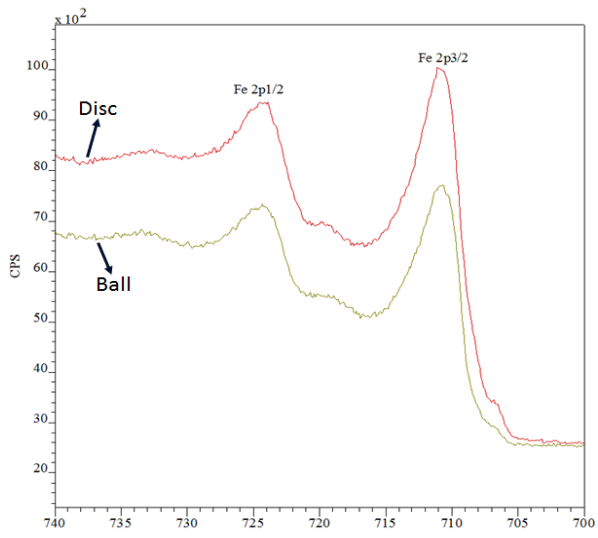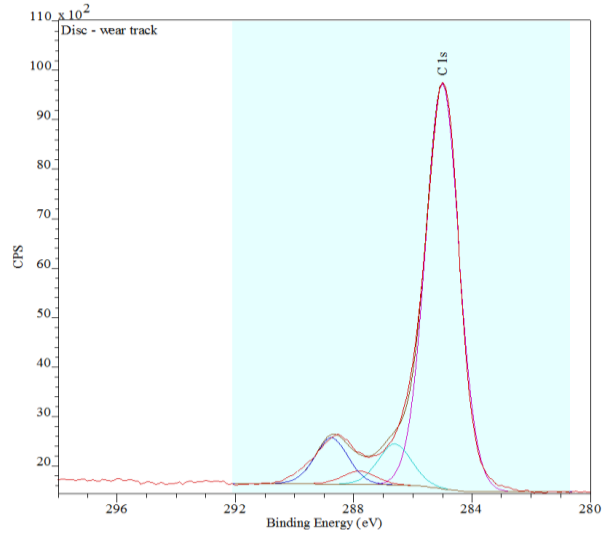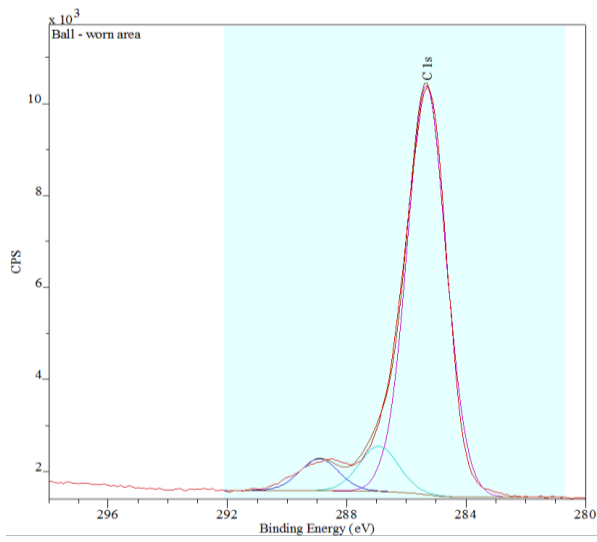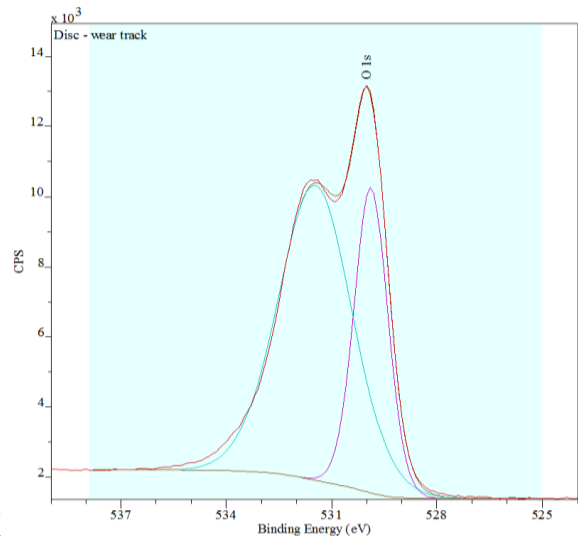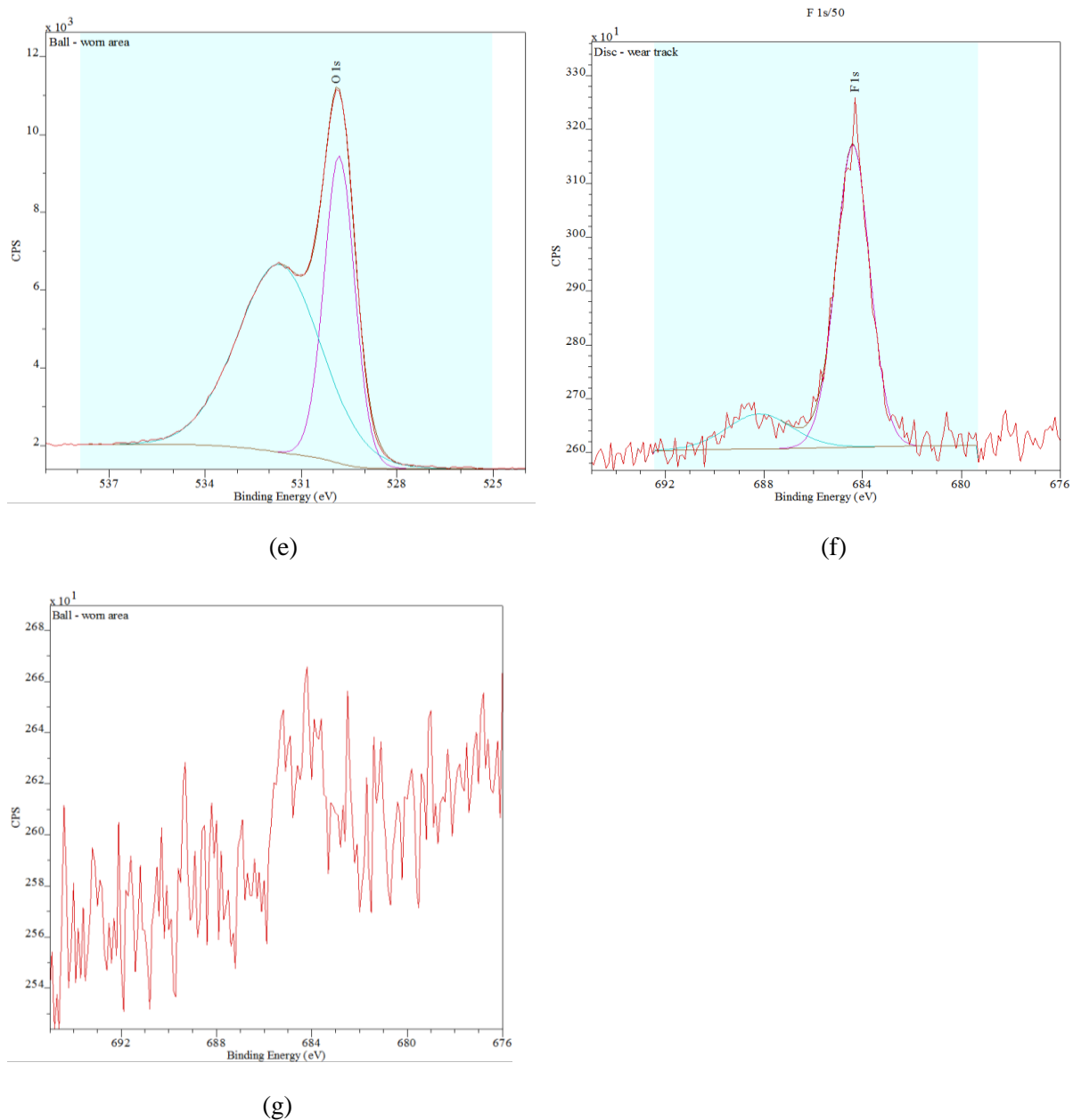
Figure 14: XPS high resolution core level spectrum: (a) Fe2p disc and ball (b) C1s disc (c) C1s ball (d) O1s disc (e) O1s ball (f) F1s disc (g) F1s ball.

The formation of an oxygenated layer in the presence of carbon dioxide [70, 77, 78] and the formation of fluorine-containing tribo-layers by various different refrigerants [8, 11, 51, 53-55, 64] have been reported to be beneficial in improving the tribological performance of rubbing surfaces. The applied normal load, mechanical motion, heat and frictional force facilitate the chemical breakdown of the refrigerant ($C_3F_7OCH_3$). C-F, Carbon-Fluorine single bonds are highly polar bonds ($C^{\delta+} - F^{\delta-}$) and C-F bond is shorter than the C-H bond which makes C-H easier to break in comparison to C-F bond [53, 79]. It has also been reported that the oxygen-carbon bond is weaker than the carbon-carbon bond [63, 80]. It is highly possible that the carbon-oxygen bond in HFE-7000 is the first bond to break which frees OCH_3 from the rest of the molecule. During the course of an experiment; material removal from the surface of EN1A steel by hard 52100 steel ball leads to the exposure of fresh surface which contains immobilised free radicals or dangling bonds. Unlike free radicals, immobilised free radicals are kinetically more stable because of their limited mobility in a solid medium. However,

similar to free radicals, immobilised free radicals are also extremely reactive. The breakdown of refrigerant and the exposure of fresh highly reactive bonds on the surface of the EN1A steel specimen leads to a chemical reaction between the refrigerant and EN1A steel. This leads to the adsorption of HFE-7000 on to the surfaces therefore forming oxygenated and fluorinated tribo-films which results in reduction in friction and wear. Besides the adhered softer material on the ball, scratch marks are also clearly visible on the surface of the ball in the contact region, which leads to a similar chemical reaction between the ball the refrigerant as well. These tribo-layers are well adhered to the rubbing surface as the presence of fluorine and oxygen was not only detected throughout the wear scar on the disc specimen but was also detected on different contact regions on the ball specimen.

7. Conclusions

A micro friction machine has been successfully modified and commissioned for bench testing the future generation of refrigerants within tribological context. A series of testes have been conducted to assess the tribological performance of the environmentally friendly refrigerant HFE-7000 by varying the tribo-operating conditions. Variable operating environments have been simulated during this study. Tests have been performed by changing the applied normal load, by using samples of various surface finish and by heating the refrigerant to various temperatures. HFE-7000 has a wide ranging application areas and the tribological performance of the refrigerant has been investigated at low loads and low temperatures starting from room temperature. The results have shown that a mechanical system based on HFE-7000 will show good friction and wear performance at higher operating temperatures and loads, in addition HFE 7000 exhibits good tribological performance at lower temperatures and low loads as well. An increase in load even at 20℃ results in a significant reduction in the friction coefficient and the increase in temperature at a low load of even 10 *N* reduces wear.

Overall the results indicate that increasing the operating temperature at a constant load reduces both friction coefficient and wear. Increasing the load at a constant temperature increases wear but results in a reduction in friction coefficient. The reduction in the friction coefficient with increasing load and decrease in wear along with a decrease in coefficient of friction with increasing temperature is believed to be associated with the development of protective tribo-films on the interacting surfaces. The formation of these films is accelerated by an elevation in the refrigerant temperature and increase in the applied load. Increasing the applied load and operating temperature increases the reactivity of the refrigerant HFE-7000 with the rubbing metals. EDS analyses on the samples in the contact region and wear track have shown a significant presence of oxygen, fluorine and carbon on the rubbing surfaces. The detailed high resolution XPS analysis reveal the formation of new bonds/compounds on the surfaces of the interacting metals and indicate breaking up of the bonds of the refrigerant. Analysis on different regions within the contact zone of the rubbing metals post-experimentation has demonstrated that oxygenated and fluorinated layers are well adhered on the disc wear track and ball. It is also observed from the results obtained that the surface roughness does not have a very significant effect on the coefficient of friction and on wear. This shows that metallic parts of a range of surface finish and even parts with rough surface finish can be used in HFE-7000 run interacting systems.

The results of this study show that HFE-7000 which is a promising future generation refrigerant from a thermodynamics point of view has demonstrated good tribological performance. It can be inferred with confidence evidenced by the results presented here, that HFE-7000 based interacting systems will show better friction and wear performance as compared to their predecessors HFCs.

Acknowledgments:

References

[1]   J.T. McMullan, *Refrigeration and the environment — issues and strategies for the future*, international Journal of Refrigeration, vol. 25, no. 1, pp. 89-99, 2002/01/01/ 2002, doi: 10.1016/S0140-7007(01)00007-X.

[2]   B. Xiang, P.K. Patra, S.A. Montzka, S.M. Miller, J.W. Elkins, F.L. Moore, E.L. Atlas, B.R. Miller, R.F. Weiss, R.G. Prinn, S.C. Wofsy, *Global emissions of refrigerants HCFC-22 and HFC-134a: Unforeseen seasonal contributions*, Proceedings of the National Academy of Sciences, vol. 111, no. 49, pp. 17379-17384, 2014, 10.1073/pnas.1417372111.

[3]   M.U. Bhutta, Z.A. Khan, N.P. Garland, A. Ghafoor, *A Historical Review on the Tribological Performance of Refrigerants used in Compressors*, Tribology in Industry, vol. 40, no. 1, pp. 19-51, 2018, 10.24874/ti.2018.40.01.03.

[4]   J.M. Calm, *The next generation of refrigerants–Historical review, considerations, and outlook*, international Journal of Refrigeration, vol. 31, no. 7, pp. 1123-1133, 2008, doi: 10.1016/j.ijrefrig.2008.01.013.

[5]   S. Jollev, *New and Unique Lubricants for Use in Compressors Utilizing R-134a Refrigerant*, in International Refrigeration and Air Conditioning Conference, Purdue University, Indiana, USA, 17-20 July, 1990, Paper 96.

[6]   B. Davis, T.K. Sheiretov, C. Cusano, *Tribological Evaluation of Contacts Lubricated by Oil-Refrigerant Mixtures*, in Air Conditioning and Refrigeration Center, College of Engineering, University of Illinois at Urbana-Champaign, USA, ACRC Technical Report 19, May 1992.

[7]   S. KOMATSUZAKI, Y. HOMMA, *Lubricants for HFC Refrigerant Compressors*, Journal of The Japan Petroleum Institute, vol. 37, no. 3, pp. 226-235, 1994, 10.1627/jpi1958.37.226.

[8]   K. Mizuhara, M. Akei, T. Matsuzaki, *The friction and wear behavior in controlled alternative refrigerant atmosphere*, Tribology Transactions, vol. 37, no. 1, pp. 120-128, 1994, 10.1080/10402009408983274.

[9]   T. Sheiretov, W.V. Glabbeek, C. Cusano, *Tribological evaluation of various surface treatments for M2 tool steel in a refrigerant environment*, in International Compressor Engineering Conference, Purdue University, Indiana, USA, 19-22 July, 1994, Paper 964.

[10]   M. Akei, K. Mizuhara, T. Taki, T. Yamamoto, *Evaluation of film-forming capability of refrigeration lubricants in pressurized refrigerant atmosphere*, Wear, vol. 196, no. 1-2, pp. 180-187, 1996, 10.1016/0043-1648(95)06917-8.

[11]   K. Kawahara, S. Mishina, A. Kamino, K. Ochiai, T. Okawa, S. Fujimoto, *Tribological Evaluation of Rotary Compressor with HFC Refrigerants*, in International Compressor Engineering Conference, Purdue University, Indiana, USA, 23-26 July, 1996, Paper 1141.

[12]   S. Fujimoto, K. Sakitani, M. Watada, *Tribology Analysis in Rolling Piston Type Compressor*, in International Compressor Engineering Conference, Purdue University, Indiana, USA, 1984, Paper 477.

[13]   M. Muraki, K. Tagawa, D. Dong, *Refrigeration Lubricant Based on Polyolester for Use With HFCs and Prospect of Its Application With R-22 (Part 1) Tribological Characteristics*, in International Refrigeration and Air Conditioning Conference, Purdue University, Indiana, USA, 23-26 July, 1996, Paper 336.

[14]   R. Tuomas, O. Isaksson, *Measurement of lubrication conditions in a rolling element bearing in a refrigerant environment*, Industrial Lubrication and Tribology, vol. 61, no. 2, pp. 91-99, 2009, 10.1108/00368790910940419.

[15]   M.J. Molina, F.S. Rowland, *Stratospheric sink for chlorofluoromethanes: chlorine atom-catalysed destruction of ozone*, Nature, vol. 249, no. 5460, pp. 810-812, 1974.

[16]   U. Nations, *Montreal Protocol on Substances that Deplete the Ozone Layer*, in United Nations Environment Programme, Montreal, Canada, 16 September 1987.

[17]   D.P. Wilson, R.S. Basu, *Thermodynamic properties of a new stratospherically safe working fluid-refrigerant 134a*, in ASHRAE transactions, 1988, pp. Pages 2095-2118.

[18]   I.R. Shankland, R.S. Basu, D.P. Wilson, *Thermal conductivity and viscosity of a new stratospherically safe refrigerant-1, 1, 1, 2-tetrafluoroethane (R-134a)*, in International Refrigeration and Air Conditioning Conference, Purdue University, Indiana, USA, 1988, Paper 41.

[19]   H. Spauschus, *HFC 134a as a substitute refrigerant for CFC 12*, international Journal of Refrigeration, vol. 11, no. 6, pp. 389-392, 1988, 10.1016/0140-7007(88)90063-1.

[20]   S.J. Eckels, M.B. Pate, *An experimental comparison of evaporation and condensation heat transfer coefficients for HFC-134a and CFC-12*, international Journal of Refrigeration, vol. 14, no. 2, pp. 70-77, 1991, 10.1016/0140-7007(91)90078-U.

[21]   S.H. Khan, S.M. Zubair, *Thermodynamic analyses of the CFC-12 and HFC-134a refrigeration cycles*, Energy, vol. 18, no. 7, pp. 717-726, 1993, 10.1016/0360-5442(93)90031-8.

[22]   S. Kitaichi, S. Sato, R. Ishidoya, T. Machida, *Tribological Analysis of Metal Interface Reactions in Lubricant Oils/CFC12 and HFC 134a System*, in International Refrigeration and Air Conditioning Conference, 17-20 July, 1990, Purdue University, Indiana, USA, paper 97.

[23]   B.C. Na, K.J. Chun, D.-C. Han, *A tribological study of refrigeration oils under HFC-134a environment*, Tribology International, vol. 30, no. 9, pp. 707-716, 1997, 10.1016/S0301-679X(97)00072-8.

[24]   Y. Yamamoto, S. Gondo, *Friction and wear characteristics of lubricants for alternative refrigerant HFC 134*, JSME International Journal Series C Mechanical Systems, Machine Elements and Manufacturing, vol. 41, no. 2, pp. 278-284, 1998, doi: 10.1299/jsmec.41.278.

[25]   M. Takesue, S. Tominaga, *Wear and Scuffing Characteristics of Polyvinylether (PVE) in an HFC Atmosphere*, in International Refrigeration and Air Conditioning Conference, 14-17 July, 1998, Purdue University, Indiana, USA, paper 440.

[26]   H. Yoon, T. Sheiretov, C. Cusano, *Tribological evaluation of some aluminum-based materials in lubricant/refrigerant mixtures*, Wear, vol. 218, no. 1, pp. 54-65, 1998, doi: 10.1016/S0043-1648(98)00195-1.

[27]   T. Sheiretov, H. Yoon, C. Cusano, *Tribological Evaluation of Various Aluminum Alloys in Lubricant/Refrigerant Mixtures*, Air Conditioning and Refrigeration Center, College of Engineering, University of Illinois at Urbana-Champaign, ACRC Technical Report 92, 1996.

[28]   C. Ciantar, M. Hadfield, A. Smith, A. Swallow, *The influence of lubricant viscosity on the wear of hermetic compressor components in HFC-134a environments*, Wear, vol. 236, no. 1, pp. 1-8, 1999, doi: 10.1016/S0043-1648(99)00267-7.

[29]   C. Ciantar, M. Hadfield, A. Swallow, A. Smith, *The influence of POE and PVE lubricant blends within hermetic refrigerating compressors operating with HFC-134a refrigerant*, Wear, vol. 241, no. 1, pp. 53-64, 2000, doi: 10.1016/S0043-1648(00)00361-6.

[30]   H. Fukui, K.-i. Sanechika, M. Ikeda, *Novel refrigeration lubricants for use with HFC refrigerants*, Tribology International, vol. 33, no. 10, pp. 707-713, 2000, doi: 10.1016/S0301-679X(00)00107-9.

[31]   Y. Yamamoto, S. Gondo, J. Kim, *Solubility of HFC134a in Lubricants and Its Influence on Tribological Performance*, Tribology Transactions, vol. 44, no. 2, pp. 209-214, 2001, doi: 10.1080/10402000108982450.

[32] C. Ciantar, M. Hadfield, *A study of tribological durability with associated environmental impacts of a domestic refrigerator*, Materials & Design, vol. 25, no. 4, pp. 331-341, 2004, doi: 10.1016/j.matdes.2003.10.016.

[33] Y.-Z. Lee, S.-D. Oh, *Friction and wear of the rotary compressor vane–roller surfaces for several sliding conditions*, Wear, vol. 255, no. 7–12, pp. 1168-1173, 2003, doi: 10.1016/S0043-1648(03)00278-3.

[34] F. Wardle, B. Jacobson, H. Dolfsma, E. Hoglund, U. Jonsson, *The effect of refrigerants on the lubrication of rolling element bearings used in screw compressors*, in International Compressor Engineering Conference, Purdue University, Indiana, USA, 14-17 July, 1992, Paper 843.

[35] B. Jacobson, *Lubrication of Screw Compressor Bearings in the Presence of Refrigerants*, in International Compressor Engineering Conference, Purdue University, Indiana, USA, 19-22 July, 1994, Paper 966.

[36] T. Hamada, N. Nishiura, *Refrigeration lubricant based on polyolester for use with HFCs and prospect of its application with R-22 (Part 2) Hydrolytic stability and compressor endurance test results*, in International Refrigeration and Air Conditioning Conference, Purdue University, Indiana, USA, 23-26 July, 1996, Paper 337.

[37] B. Jacobson, *Ball Bearing Lubrication in Refrigetation Compressors*, in International Compressor Engineering Conference, Purdue University, Indiana, USA, 23-26 July, 1996, Paper 1090.

[38] M. Akei, K. Mizuhara, *The Elastohydrodynamic Properties of Lubricants in Refrigerant Environments©*, Tribology Transactions, vol. 40, no. 1, pp. 1-10, 1997, 10.1080/10402009708983622.

[39] B.O. Jacobson, G.E.M. Espejel, *High pressure investigation of refrigerants HFC245fa, R134a and R123*, in International Compressor Engineering Conference, Purdue University, Indiana, USA, 17-20 July, 2006, Paper 1789.

[40] R. Tuomas, O. Isaksson, *Compressibility of Oil/Refrigerant Lubricants in Elasto-Hydrodynamic Contacts*, Journal of Tribology, vol. 128, no. 1, pp. 218-220, 2005, 10.1115/1.2125967.

[41] C. Breidenich, D. Magraw, A. Rowley, J.W. Rubin, *The Kyoto protocol to the United Nations framework convention on climate change*, American Journal of International Law, vol. 92, no. 2, pp. 315-331, 1998, doi: 10.2307/2998044.

[42] N. Garland, M. Hadfield, *Environmental implications of hydrocarbon refrigerants applied to the hermetic compressor*, Materials & Design, vol. 26, no. 7, pp. 578-586, 2005, 10.1016/j.matdes.2004.08.009.

[43] Z.A. Khan, M. Hadfield, Y. Wang, *Pressurised chamber design for conducting rolling contact experiments with liquid refrigerant lubrication*, Materials & Design, vol. 26, no. 8, pp. 680-689, 2005, 10.1016/j.matdes.2004.08.006.

[44] Z.A. Khan, M. Hadfield, S. Tobe, Y. Wang, *Ceramic rolling elements with ring crack defects—A residual stress approach*, Materials Science and Engineering: A, vol. 404, no. 1, pp. 221-226, 2005, 10.1016/j.msea.2005.05.087.

[45] Z.A. Khan, M. Hadfield, S. Tobe, Y. Wang, *Residual stress variations during rolling contact fatigue of refrigerant lubricated silicon nitride bearing elements*, Ceramics international, vol. 32, no. 7, pp. 751-754, 2006, 10.1016/j.ceramint.2005.05.012.

[46] Z.A. Khan, M. Hadfield, *Manufacturing induced residual stress influence on the rolling contact fatigue life performance of lubricated silicon nitride bearing materials*, Materials & Design, vol. 28, no. 10, pp. 2688-2693, 2007, 10.1016/j.matdes.2006.10.003.

[47] K. Sariibrahimoglu, H. Kizil, M.F. Aksit, I. Efeoglu, H. Kerpicci, *Effect of R600a on tribological behavior of sintered steel under starved lubrication*, Tribology International, vol. 43, no. 5, pp. 1054-1058, 2010, 10.1016/j.triboint.2009.12.035.

[48] J. De Mello, R. Binder, N. Demas, A. Polycarpou, *Effect of the actual environment present in hermetic compressors on the tribological behaviour of a Si-rich multifunctional DLC coating*, Wear*,* vol. 267, no. 5, pp. 907-915, 2009, doi: 10.1016/j.wear.2008.12.070.

[49] T.A. Solzak, A.A. Polycarpou, *Tribology of hard protective coatings under realistic operating conditions for use in oilless piston-type and swash-plate compressors*, Tribology Transactions*,* vol. 53, no. 3, pp. 319-328, 2010, 10.1080/10402000903283300.

[50] M. Spatz, B. Minor, H. DuPont, *HFO-1234yf A low GWP refrigerant for MAC. Honeywell/DuPont joint collaboration*, in SAE World Congress 14-17 April, 2008, Detroit, Michigan, USA.

[51] H.N. Tatsuya Sasaki, Hideaki Maeyama, Kota Mizuno, *Tribology Characteristics of HFO and HC Refrigerants with Immiscible Oils - Effect of Refrigerant with Unsaturated Bond*, in International Compressor Engineering Conference, Purdue University, Indiana, USA, 12-15 July, 2010, Paper 1946.

[52] S.P. Mishra, A.A. Polycarpou, *Tribological studies of unpolished laser surface textures under starved lubrication conditions for use in air-conditioning and refrigeration compressors*, Tribology International*,* vol. 44, no. 12, pp. 1890-1901, 2011, 10.1016/j.triboint.2011.08.005.

[53] M.W. Akram, K. Polychronopoulou, A.A. Polycarpou, *Lubricity of environmentally friendly HFO-1234yf refrigerant*, Tribology International*,* vol. 57, pp. 92-100, 2013, 10.1016/j.triboint.2012.07.013.

[54] M.W. Akram, K. Polychronopoulou, C. Seeton, A.A. Polycarpou, *Tribological performance of environmentally friendly refrigerant HFO-1234yf under starved lubricated conditions*, Wear*,* vol. 304, no. 1, pp. 191-201, 2013, 10.1016/j.wear.2013.04.035.

[55] M.W. Akram, K. Polychronopoulou, A.A. Polycarpou, *Tribological performance comparing different refrigerant–lubricant systems: The case of environmentally friendly HFO-1234yf refrigerant*, Tribology International*,* vol. 78, pp. 176-186, 2014, 10.1016/j.triboint.2014.05.015.

[56] M.W. Akram, J.L. Meyer, A.A. Polycarpou, *Tribological interactions of advanced polymeric coatings with polyalkylene glycol lubricant and r1234yf refrigerant*, Tribology International*,* vol. 97, pp. 200-211, 2016, 10.1016/j.triboint.2016.01.026.

[57] R.J. Hulse, R.S. Basu, R.R. Singh, R.H. Thomas, *Physical properties of HCFO-1233zd (E)*, Journal of Chemical & Engineering Data*,* vol. 57, no. 12, pp. 3581-3586, 2012, doi: 10.1021/je300776s.

[58] (3M™ Novec™ 7000 Engineered Fluid). Data sheet [https://multimedia.3m.com/mws/media/121372O/3m-novec-7000-engineered-fluid-tds.pdf].

[59] R. Akasaka, Y. Kayukawa, *A fundamental equation of state for trifluoromethyl methyl ether (HFE-143m) and its application to refrigeration cycle analysis*, international Journal of Refrigeration*,* vol. 35, no. 4, pp. 1003-1013, 2012, doi: org/10.1016/j.ijrefrig.2012.01.003.

[60] H. Helvaci, Z.A. Khan, *Experimental study of thermodynamic assessment of a small scale solar thermal system*, Energy Conversion and Management*,* vol. 117, pp. 567-576, 2016, 10.1016/j.enconman.2016.03.050.

[61] H.U. Helvaci, Z.A. Khan, *Heat transfer and entropy generation analysis of HFE 7000 based nanorefrigerants*, International Journal of Heat and Mass Transfer*,* vol. 104, pp. 318-327, 2017/01/01 2017, 10.1016/j.ijheatmasstransfer.2016.08.053.

[62] A. Sekiya, S. Misaki, *The potential of hydrofluoroethers to replace CFCs, HCFCs and PFCs*, Journal of Fluorine Chemistry*,* vol. 101, no. 2, pp. 215-221, 2000/02/01/ 2000, doi: 10.1016/S0022-1139(99)00162-1.

[63] M. Muraki, T. Sano, D. Dong, *Elastohydrodynamic properties and boundary lubrication performance of polyolester in a hydrofluoroether refrigerant environment*, Proceedings of the Institution of Mechanical Engineers, Part J: Journal of Engineering Tribology*,* vol. 216, no. 1, pp. 19-26, 2002, doi: 10.1243/1350650021543852.

[64] M. Bhutta, Z. Khan, N. Garland, *Wear Performance Analysis of Ni–Al$_2$O$_3$ Nanocomposite Coatings under Nonconventional Lubrication*, Materials, vol. 12, no. 1, p. 36, 2018, doi: 10.3390/ma12010036.

[65] P. Vergne, N. Fillot, N. Bouscharain, N. Devaux, G.E. Morales-Espejel, *An experimental and modeling assessment of the HCFC-R123 refrigerant capabilities for lubricating rolling EHD circular contacts*, Proceedings of the Institution of Mechanical Engineers, Part J: Journal of Engineering Tribology, vol. 229, no. 8, pp. 950-961, 2015, doi: 10.1177/1350650115574537.

[66] M.L. Cannaday, A.A. Polycarpou, *Tribology of unfilled and filled polymeric surfaces in refrigerant environment for compressor applications*, Tribology Letters, vol. 19, no. 4, pp. 249-262, 2005, doi: 10.1007/s11249-005-7441-9.

[67] S.M. Yeo, A.A. Polycarpou, *Fretting experiments of advanced polymeric coatings and the effect of transfer films on their tribological behavior*, Tribology International, vol. 79, pp. 16-25, 2014, doi: 10.1016/j.triboint.2014.05.012.

[68] T.A. Solzak, A.A. Polycarpou, *Tribology of protective hard coatings for use in oil-less, piston-type compressors*, in International Compressor Engineering Conference, Purdue University, Indiana, USA, 17-20 July, 2006, Paper 1790.

[69] N.G. Demas, A.A. Polycarpou, *Tribological investigation of cast iron air-conditioning compressor surfaces in CO$_2$ refrigerant*, Tribology Letters, vol. 22, no. 3, pp. 271-278, 2006, 10.1007/s11249-006-9094-8.

[70] E.E. Nunez, K. Polychronopoulou, A.A. Polycarpou, *Lubricity effect of carbon dioxide used as an environmentally friendly refrigerant in air-conditioning and refrigeration compressors*, Wear, vol. 270, no. 1, pp. 46-56, 2010, 10.1016/j.wear.2010.09.005.

[71] B.H. Minor, D. Herrmann, R. Gravell, *Flammability characteristics of HFO-1234yf*, Process Safety Progress, vol. 29, no. 2, pp. 150-154, 2009, doi: 10.1002/prs.10347.

[72] Global Warming Potential Values, https://www.ghgprotocol.org/sites/default/files/ghgp/Global-Warming-Potential-Values%20%28Feb%2016%202016%29_1.pdf.

[73] Spectroscopy: http://www.spectroscopyonline.com/xps-surface-characterization-disposable-laboratory-gloves-and-transfer-glove-components-other-surfac.

[74] Thermo Scientific XPS , https://xpssimplified.com/periodictable.php.

[75] X-ray Photoelectron Spectroscopy (XPS) Reference Pages, http://www.xpsfitting.com/.

[76] X. Wu, P. Cong, H. Nanao, I. Minami, S. Mori, *Tribological behaviors of 52100 steel in carbon dioxide atmosphere*, Tribology Letters, vol. 17, no. 4, pp. 925-930, 2004, 10.1007/s11249-004-8101-1.

[77] H.-G. Jeon, S.-D. Oh, Y.-Z. Lee, *Friction and wear of the lubricated vane and roller materials in a carbon dioxide refrigerant*, Wear, vol. 267, no. 5, pp. 1252-1256, 2009, 10.1016/j.wear.2008.12.097.

[78] M. Cannaday, A. Polycarpou, *Advantages of CO$_2$ compared to R410a refrigerant of tribologically tested Aluminum 390-T6 surfaces*, Tribology Letters, vol. 21, no. 3, pp. 185-192, 2006, 10.1007/s11249-005-9013-4.

[79] G. Gu, Z. Wu, Z. Zhang, F. Qing, *Tribological properties of fluorine-containing additives of silicone oil*, Tribology International, vol. 42, no. 3, pp. 397-402, 2009/03/01/ 2009, doi: 10.1016/j.triboint.2008.07.012.

[80] D.R. Lide, *CRC handbook of chemistry and physics,* : CRC Press, Boca Raton, Florida, 73rd edition, 1992-1993, pp. 9-145.